IEC TR 63307

Edition 1.0 2020-11

TECHNICAL REPORT

colour inside

Measurement methods of the complex relative permeability and permittivity of noise suppression sheet

IECNORM.COM : Click to view the full PDF of IEC TR 63307:2020

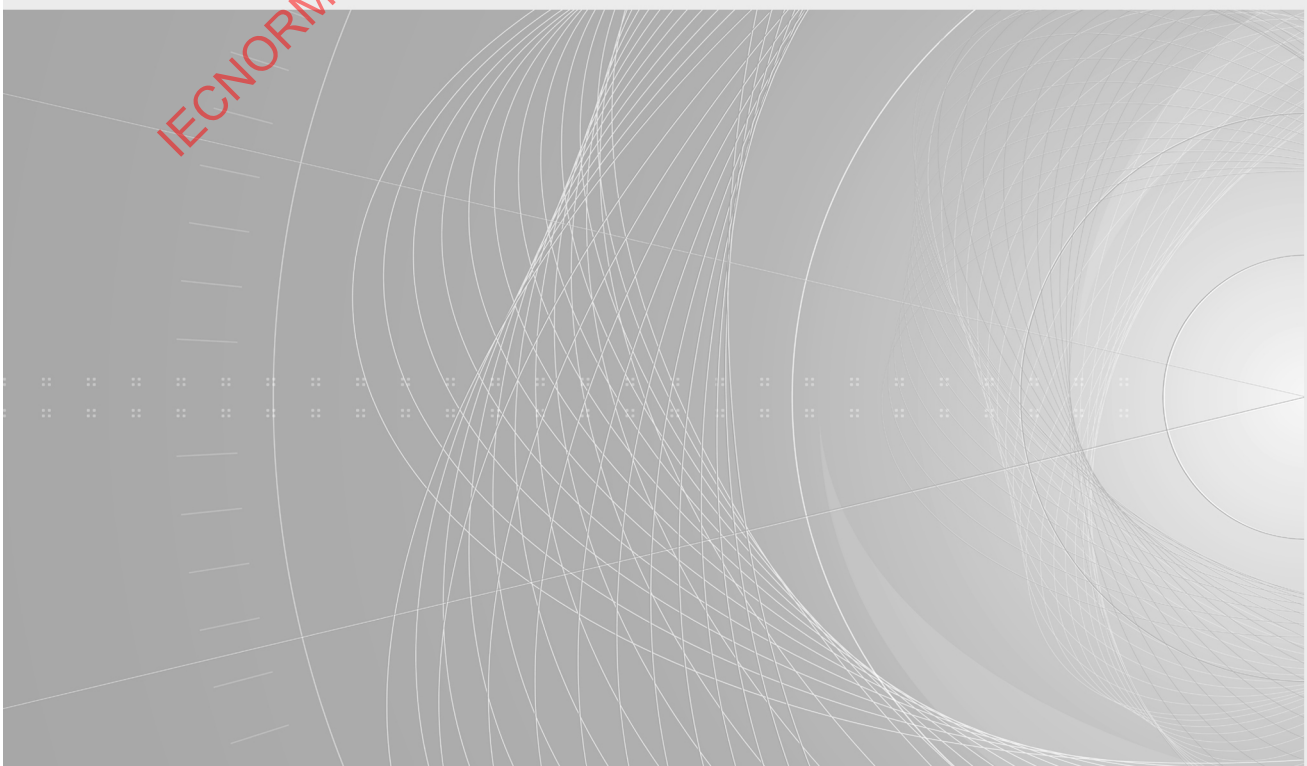

IEC TR 63307:2020-11(en)

THIS PUBLICATION IS COPYRIGHT PROTECTED
Copyright © 2020 IEC, Geneva, Switzerland

All rights reserved. Unless otherwise specified, no part of this publication may be reproduced or utilized in any form or by any means, electronic or mechanical, including photocopying and microfilm, without permission in writing from either IEC or IEC's member National Committee in the country of the requester. If you have any questions about IEC copyright or have an enquiry about obtaining additional rights to this publication, please contact the address below or your local IEC member National Committee for further information.

IEC Central Office
3, rue de Varembé
CH-1211 Geneva 20
Switzerland

Tel.: +41 22 919 02 11
info@iec.ch
www.iec.ch

About the IEC
The International Electrotechnical Commission (IEC) is the leading global organization that prepares and publishes International Standards for all electrical, electronic and related technologies.

About IEC publications
The technical content of IEC publications is kept under constant review by the IEC. Please make sure that you have the latest edition, a corrigendum or an amendment might have been published.

IEC publications search - webstore.iec.ch/advsearchform
The advanced search enables to find IEC publications by a variety of criteria (reference number, text, technical committee,…). It also gives information on projects, replaced and withdrawn publications.

IEC Just Published - webstore.iec.ch/justpublished
Stay up to date on all new IEC publications. Just Published details all new publications released. Available online and once a month by email.

IEC Customer Service Centre - webstore.iec.ch/csc
If you wish to give us your feedback on this publication or need further assistance, please contact the Customer Service Centre: sales@iec.ch.

Electropedia - www.electropedia.org
The world's leading online dictionary on electrotechnology, containing more than 22 000 terminological entries in English and French, with equivalent terms in 16 additional languages. Also known as the International Electrotechnical Vocabulary (IEV) online.

IEC Glossary - std.iec.ch/glossary
67 000 electrotechnical terminology entries in English and French extracted from the Terms and Definitions clause of IEC publications issued since 2002. Some entries have been collected from earlier publications of IEC TC 37, 77, 86 and CISPR.

IECNORM.COM : Click to view the full PDF of IEC TR 63307:2020

IEC TR 63307

Edition 1.0 2020-11

TECHNICAL REPORT

IECNORM.COM : Click to view the full PDF of IEC TR 63307:2020

colour inside

Measurement methods of the complex relative permeability and permittivity of noise suppression sheet

INTERNATIONAL
ELECTROTECHNICAL
COMMISSION

ICS 29.100.10

ISBN 978-2-8322-9085-9

Warning! Make sure that you obtained this publication from an authorized distributor.

® Registered trademark of the International Electrotechnical Commission

CONTENTS

IECNORM.COM : Click to view the full PDF of IEC TR 63307:2020

IECNORM.COM : Click to view the full PDF of IEC TR 63307:2020

IECNORM.COM : Click to view the full PDF of IEC TR 63307:2020

IECNORM.COM : Click to view the full PDF of IEC TR 63307:2020

INTERNATIONAL ELECTROTECHNICAL COMMISSION

_____

MEASUREMENT METHODS OF THE COMPLEX RELATIVE PERMEABILITY AND PERMITTIVITY OF NOISE SUPPRESSION SHEET

FOREWORD

1) The International Electrotechnical Commission (IEC) is a worldwide organization for standardization comprising all national electrotechnical committees (IEC National Committees). The object of IEC is to promote international co-operation on all questions concerning standardization in the electrical and electronic fields. To this end and in addition to other activities, IEC publishes International Standards, Technical Specifications, Technical Reports, Publicly Available Specifications (PAS) and Guides (hereafter referred to as "IEC Publication(s)"). Their preparation is entrusted to technical committees; any IEC National Committee interested in the subject dealt with may participate in this preparatory work. International, governmental and non-governmental organizations liaising with the IEC also participate in this preparation. IEC collaborates closely with the International Organization for Standardization (ISO) in accordance with conditions determined by agreement between the two organizations.
2) The formal decisions or agreements of IEC on technical matters express, as nearly as possible, an international consensus of opinion on the relevant subjects since each technical committee has representation from all interested IEC National Committees.
3) IEC Publications have the form of recommendations for international use and are accepted by IEC National Committees in that sense. While all reasonable efforts are made to ensure that the technical content of IEC Publications is accurate, IEC cannot be held responsible for the way in which they are used or for any misinterpretation by any end user.
4) In order to promote international uniformity, IEC National Committees undertake to apply IEC Publications transparently to the maximum extent possible in their national and regional publications. Any divergence between any IEC Publication and the corresponding national or regional publication shall be clearly indicated in the latter.
5) IEC itself does not provide any attestation of conformity. Independent certification bodies provide conformity assessment services and, in some areas, access to IEC marks of conformity. IEC is not responsible for any services carried out by independent certification bodies.
6) All users should ensure that they have the latest edition of this publication.
7) No liability shall attach to IEC or its directors, employees, servants or agents including individual experts and members of its technical committees and IEC National Committees for any personal injury, property damage or other damage of any nature whatsoever, whether direct or indirect, or for costs (including legal fees) and expenses arising out of the publication, use of, or reliance upon, this IEC Publication or any other IEC Publications.
8) Attention is drawn to the Normative references cited in this publication. Use of the referenced publications is indispensable for the correct application of this publication.
9) Attention is drawn to the possibility that some of the elements of this IEC Publication may be the subject of patent rights. IEC shall not be held responsible for identifying any or all such patent rights.

The main task of IEC technical committees is to prepare International Standards. However, a technical committee may propose the publication of a technical report when it has collected data of a different kind from that which is normally published as an International Standard, for example "state of the art".

IEC TR 63307, which is a technical report, has been prepared by IEC technical committee 51: Magnetic components, ferrite and magnetic powder materials.

The text of this Technical Specification is based on the following documents:

Draft TR	Report on voting
51/1349/DTR	51/1356/RVDTR

Full information on the voting for its approval can be found in the report on voting indicated in the above table.

The language used for the development of this Technical Report is English.

IECNORM.COM : Click to view the full PDF of IEC TR 63307:2020

This document was drafted in accordance with ISO/IEC Directives, Part 2, and developed in accordance with ISO/IEC Directives, Part 1 and ISO/IEC Directives, IEC Supplement, available at www.iec.ch/members_experts/refdocs. The main document types developed by IEC are described in greater detail at www.iec.ch/standardsdev/publications.

The committee has decided that the contents of this document will remain unchanged until the stability date indicated on the IEC website under "http://webstore.iec.ch" in the data related to the specific document. At this date, the document will be

- reconfirmed,
- withdrawn,
- replaced by a revised edition, or
- amended.

IMPORTANT – The 'colour inside' logo on the cover page of this publication indicates that it contains colours which are considered to be useful for the correct understanding of its contents. Users should therefore print this document using a colour printer.

IECNORM.COM : Click to view the full PDF of IEC TR 63307:2020

INTRODUCTION

Noise suppression sheet (NSS) is used near the source of high frequency electromagnetic noise, path of noise propagation and source of emission. It is used like a patch and is different from an electromagnetic wave absorber in free space. IEC 62333-2 specifies five measurement methods in order to estimate the effect of NSS. To evaluate the effect by computer simulation, it is indispensable to know the frequency characteristics of both permeability and permittivity. And to make a rough estimate of the noise suppression effect of NSS, it is useful to understand effective permeability and effective permittivity, which are the permeability and permittivity of an actually used shape.

As most NSSs are flexible, and both complex relative permeability and complex relative permittivity have anisotropy, careful study and understanding of the principles are indispensable for the measurement of the frequency characteristics of permeability and permittivity.

There are various methods to measure permeability and permittivity under the frequency range where NSS is used. This document is intended to be used for the proper selection of the measurement method and the preparation of the test sample to achieve the above purpose when measuring permeability and permittivity, the two parameters which largely influence the noise suppression effect of the NSS.

IECNORM.COM : Click to view the full PDF of IEC TR 63307:2020

MEASUREMENT METHODS OF THE COMPLEX RELATIVE PERMEABILITY AND PERMITTIVITY OF NOISE SUPPRESSION SHEET

1 Scope

This document provides guidelines on the methods for measuring the frequency characteristics of permeability and permittivity in the frequency range of 1 MHz to 6 GHz for a noise suppression sheet for each electromagnetic noise countermeasure.

2 Normative references

There are no normative references in this document.

3 Terms, definitions and symbols

3.1 Terms and definitions

For the purposes of this document, the following terms and definitions apply.

ISO and IEC maintain terminological databases for use in standardization at the following addresses:

- IEC Electropedia: available at http://www.electropedia.org/
- ISO Online browsing platform: available at http://www.iso.org/obp

3.1.1
noise suppression
suppression which consists of signal decoupling, radiation suppression and attenuation of the transmission power of noise by an electronic product

Note 1 to entry: Each function above is achieved by absorption and/or shielding.

3.1.2
noise suppression sheet
NSS
sheet which enables noise suppression and is composed of magnetic, dielectric or conductive material with electromagnetic losses

EXAMPLE Sheet made of soft magnetic metal powder and resin or rubber.

3.1.3
suppression ratio
ratio of the noise level with and without suppression sheets

Note 1 to entry: The suppression ratio is classified into intra-decoupling ratio, inter-decoupling ratio, transmission attenuation power ratio and radiation suppression ratio. It is expressed in dB.

3.2 Symbols

μ_r	complex relative permeability
μ_r'	real part of complex relative permeability
μ_r''	imaginary part of complex relative permeability
ε_r	complex relative permittivity

IECNORM.COM : Click to view the full PDF of IEC TR 63307:2020

ε'_r	real part of complex relative permittivity
ε''_r	imaginary part of complex relative permittivity
Z	impedance (Ω)
$\omega = 2\pi f$	angular frequency (rad/s)
I	current (A)
$B = \mu_0\mu_r H$	magnetic flux density (T)
H	magnetic field strength (A/m)
μ_0	permeability of vacuum ($4\pi \times 10^{-7}$ H/m)
f	frequency

4 General

Composite materials made by embedding magnetic metal flakes in a plastic sheet are widely used in PCs or mobile phone handsets. This sheet is well known as a noise suppression sheet (NSS) and is used to reduce unwanted signals in transmission lines or unwanted couplings between circuit elements in the devices described above.

Electromagnetic compatibility (EMC) designers recently have been using simulations for the design of the circuit boards for PCs and mobile phone handsets. In these simulations, it is important to know the complex relative permeability μ_r and the complex relative permittivity ε_r of NSS. This document shows the six measurement methods of μ_r and ε_r of NSS. The measurement frequency range is from 1 MHz to 6 GHz, as shown in Table 1. Figure 1 illustrates the in-plane and perpendicular measurement direction of Table 1.

Table 1 – Measurement method and frequency

Method Name	μ_r and ε_r				Frequency				
	In-plane		Perpendicular						
	μ_r	ε_r	μ_r	ε_r	1 MHz to 10 MHz	100 MHz	1 GHz	10 GHz	100 GHz
5.1 Inductance	○				1 MHz to 1 GHz				
5.2 Nicolson Ross Weir	○	○						500 MHz to	
5.3 Short-circuited micro strip line	○						10 MHz to 10 GHz		
5.4 Short-circuited coaxial line	○	○					1 MHz to 18 GHz		
5.5 Shielded loop coil	○						1 MHz to 10 GHz		
5.6 Harmonic resonance cavity perturbation	○		○					250 MHz to 18 GHz	
		○		○				1,8 MHz	

Range of frequency (1 MHz to 6 GHz)

IECNORM.COM : Click to view the full PDF of IEC TR 63307:2020

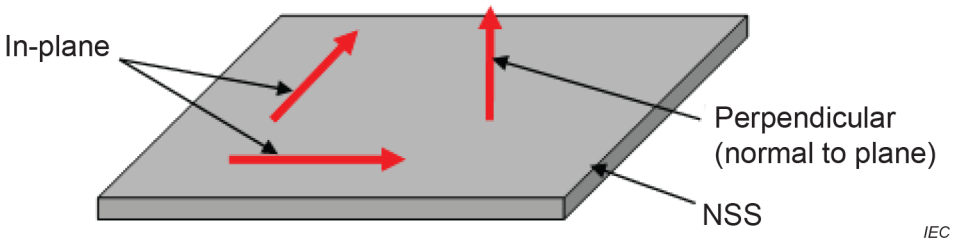

Figure 1 – In-plane and perpendicular measurement direction of NSS sample

5 Measurement methods

5.1 Inductance method

5.1.1 Measurement parameters

The measurement parameters of a magnetic material are defined as follows:

$$\mu_r = \mu_r' - j\mu_r'' \quad (1)$$

where

μ_r' and μ_r'' are the real part and the imaginary part of the complex relative permeability, respectively.

5.1.2 Measurement frequency and accuracy

The objective of this method is to evaluate the in-plane permeability of toroidal-shaped thin NSS samples shown in Figure 2 and is applicable for the measurements under the following conditions:

frequency	:	1 MHz ≤ f ≤ 1 GHz
relative permeability	:	1 ≤ μ_r' ≤ 1 000
		0 ≤ μ_r'' ≤ 1 000
accuracy	:	value error ±20 % for μ_r'
		value error ±20 % for μ_r''

The measurement frequency range is affected by the dimensions and the permeability values of the NSS sample. The higher the permittivity, the lower the upper limit of the frequency range will be.

IECNORM.COM : Click to view the full PDF of IEC TR 63307:2020

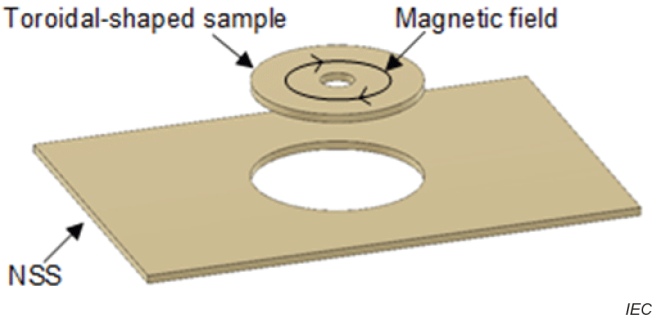

Figure 2 – Toroidal-shaped sample cut from the NSS

5.1.3 Measurement principle

The test fixture shown in Figure 3 forms the ideal one-turn inductor. The self-inductance is given by

$$\frac{Z}{\mathrm{j}\omega} = \frac{1}{I}\int_S B\, ds \tag{2}$$

where

Z is the impedance (Ω);

$\omega = 2\pi f$ is the angular frequency (rad/s);

I is the current (A);

$B = \mu_0\mu_r H$ is the magnetic flux density (T);

H is the Magnetic field strength (A/m);

μ_0 is the permeability of vacuum ($4\pi \times 10^{-7}$ H/m);

S is the surface shown in Figure 3.

Therefore, the complex relative permeability is

$$\mu_\mathrm{r} = \frac{2\pi}{\mu_0}\frac{Z_\mathrm{m} - Z_\mathrm{sm}}{\mathrm{j}\omega \mathrm{F}} + 1 = \frac{2\pi}{\mu_0}\frac{Z_\mathrm{NSS}}{\mathrm{j}\omega \mathrm{F}} + 1 \tag{3}$$

or

$$\mu_\mathrm{r}' = \frac{2\pi}{\mu_0}\frac{x_\mathrm{m} - x_\mathrm{sm}}{\omega \mathrm{F}} + 1 = \frac{2\pi}{\mu_0}\frac{x_\mathrm{NSS}}{\omega \mathrm{F}} + 1 \tag{4}$$

$$\mu_\mathrm{r}'' = \frac{2\pi}{\mu_0}\frac{r_\mathrm{m} - r_\mathrm{sm}}{\omega \mathrm{F}} = \frac{2\pi}{\mu_0}\frac{r_\mathrm{NSS}}{\omega \mathrm{F}} \tag{5}$$

where

$Z_\mathrm{m} = r_\mathrm{m} + \mathrm{j}x_\mathrm{m}$ is the measured impedance with a sample;

$Z_\mathrm{sm} = r_\mathrm{sm} + \mathrm{j}x_\mathrm{sm}$ is the measured impedance without a sample (in short state);

$Z_\mathrm{NSS} = r_\mathrm{NSS} + \mathrm{j}x_\mathrm{NSS}$ is the impedance of a NSS sample;

IECNORM.COM : Click to view the full PDF of IEC TR 63307:2020

$F = t \ln\left(\frac{b}{a}\right)$ is the shape factor of a sample, inner diameter a, outer diameter b, and thickness t.

Z_{sm} is used to minimize errors due to residual impedance by compensation. The equivalent circuit model of the test fixture is shown in Figure 4. $g_p + jb_p$ is the admittance of the test fixture and its effect can be neglected in a simplified case. Therefore, the impedance Z_{NSS} of a NSS sample is $Z_m - Z_{sm}$.

The derivation procedure is shown in detail in Annex A.

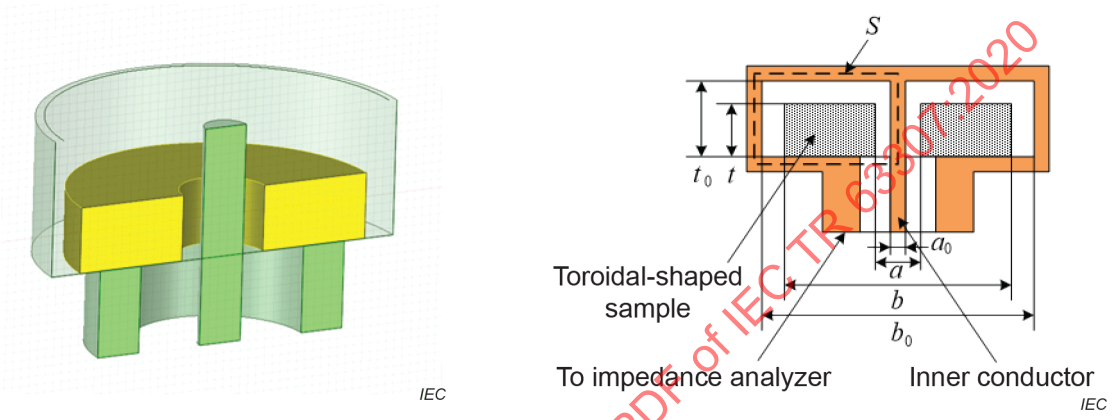

a) Structure b) Parameters

Figure 3 – Test fixture with a toroidal-shaped NSS sample

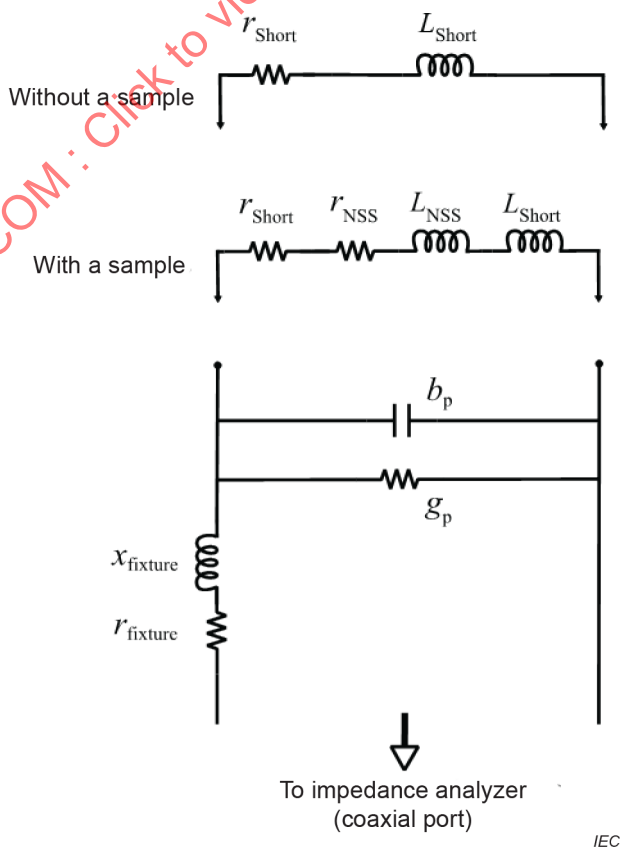

Figure 4 – Equivalent circuit model of the test fixture

IECNORM.COM : Click to view the full PDF of IEC TR 63307:2020

5.1.4 Test sample

The sample shall be fabricated in the shape of a toroidal ring. A good round sample can be obtained by a punching tool. The preferable sample size is as follows:

For the fixture of 24 mm diameter in 5.1.5:

inner diameter : $a \geq 3{,}1$ mm
outer diameter : $b \leq 8$ mm
thickness : $t \leq 3$ mm

For the fixture of 30 mm diameter:

inner diameter : $a \geq 5$ mm
outer diameter : $b \leq 20$ mm
thickness : $t \leq 8{,}5$ mm

Each parameter should be measured with a precision of less than 1/100 mm using a micrometer.

5.1.5 Test fixture

The structure of the test fixture is shown in Figure 3. The test fixture is a conductive shield surrounding the central conductor and terminates in a short circuit. The connector of the test fixture is connected through the coaxial connector to the measurement equipment. The alignment error of the NSS sample from the centre affects the measurement results, so the use of a sample holder is recommended to place a sample coaxially. Examples of features of a test fixture are as follows:

diameter : $b_0 = 24$ mm
height : $t_0 = 30$ mm
resistance : $r_{sm} = 100$ mΩ
inductance : $x_{sm}/\omega = 1{,}0$ nH

or

diameter : $b_0 = 30$ mm
height : $t_0 = 35$ mm
resistance : $r_{sm} = 300$ mΩ
inductance : $x_{sm}/\omega = 5{,}5$ nH

The diameter of a centre conductor is $a_0 = 3$ mm for both fixtures.

5.1.6 Measurement environment

The fixture and the samples shall be kept in a clean and dry state. The room temperature and the relative humidity shall preferably be 23 °C ± 5 °C and less than 60 %.

5.1.7 Measurement uncertainty

Measurement uncertainties of u_r' and μ_r'', $u(\mu_r')$ and $u(\mu_r'')$, are estimated as the combined standard uncertainty and given respectively by

IECNORM.COM : Click to view the full PDF of IEC TR 63307:2020

$$u(\mu_r')^2 = \left(\frac{\partial \mu_r'}{\partial x_m}\right)^2 u(x_m)^2 + \left(\frac{\partial \mu_r'}{\partial x_{sm}}\right)^2 u(x_{sm})^2 + \left(\frac{\partial \mu_r'}{\partial a}\right)^2 u(a)^2 + \left(\frac{\partial \mu_r'}{\partial b}\right)^2 u(b)^2 + \left(\frac{\partial \mu_r'}{\partial t}\right)^2 u(t)^2 \quad (6)$$

$$u(\mu_r'')^2 = \left(\frac{\partial \mu_r''}{\partial r_m}\right)^2 u(r_m)^2 + \left(\frac{\partial \mu_r''}{\partial r_{sm}}\right)^2 u(r_{sm})^2 + \left(\frac{\partial \mu_r''}{\partial a}\right)^2 u(a)^2 + \left(\frac{\partial \mu_r''}{\partial b}\right)^2 u(b)^2 + \left(\frac{\partial \mu_r''}{\partial t}\right)^2 u(t)^2 \quad (7)$$

where $u(x_m)$, $u(x_{sm})$, $u(r_m)$, $u(r_{sm})$, $u(a)$, $u(b)$ and $u(t)$ are standard uncertainties of x_m, x_{sm}, r_m, r_{sm}, a, b and t, respectively. The sensitivity coefficients in Formulae (6) and (7) are as follows:

$$\frac{\partial \mu_r'}{\partial x_m} = \frac{2\pi}{\mu_0}\frac{1}{\omega F} \quad (8)$$

$$\frac{\partial \mu_r'}{\partial x_{sm}} = \frac{2\pi}{\mu_0}\left(-\frac{1}{\omega F}\right) \quad (9)$$

$$\frac{\partial \mu_r'}{\partial a} = \frac{2\pi}{\mu_0}\frac{x_m - x_{sm}}{\omega}\frac{t}{a F^2} \quad (10)$$

$$\frac{\partial \mu_r'}{\partial b} = \frac{2\pi}{\mu_0}\frac{x_m - x_{sm}}{\omega}\left(-\frac{t}{b F^2}\right) \quad (11)$$

$$\frac{\partial \mu_r'}{\partial h} = \frac{2\pi}{\mu_0}\frac{x_m - x_{sm}}{\omega}\left(-\frac{1}{t F}\right) \quad (12)$$

$$\frac{\partial \mu_r''}{\partial r_m} = \frac{2\pi}{\mu_0}\frac{1}{\omega F} \quad (13)$$

$$\frac{\partial \mu_r''}{\partial r_{sm}} = \frac{2\pi}{\mu_0}\left(-\frac{1}{\omega F}\right) \quad (14)$$

$$\frac{\partial \mu_r''}{\partial a} = \frac{2\pi}{\mu_0}\frac{r_m - r_{sm}}{\omega}\frac{t}{a F^2} \quad (15)$$

$$\frac{\partial \mu_r''}{\partial b} = \frac{2\pi}{\mu_0}\frac{r_m - r_{sm}}{\omega}\left(-\frac{t}{b F^2}\right) \quad (16)$$

$$\frac{\partial \mu_r''}{\partial h} = \frac{2\pi}{\mu_0}\frac{r_m - r_{sm}}{\omega}\left(-\frac{1}{t F}\right) \quad (17)$$

IECNORM.COM : Click to view the full PDF of IEC TR 63307:2020

5.1.8 Measurement system

Figure 5 shows a schematic diagram of the measurement system. For the measurement of the magnetic properties, the information on the ratio of the current and voltage values and the phase difference between current and voltage are needed. An impedance analyzer, LCR meter or vector network analyzer (VNA) can be used for the measurement.

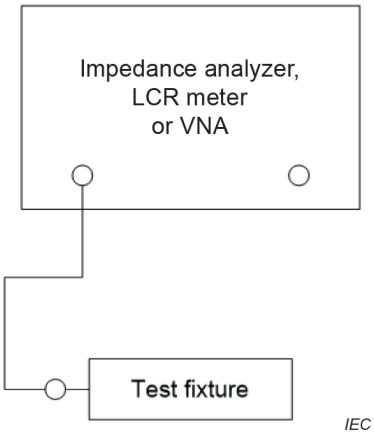

Figure 5 – Schematic diagram of measurement system

5.1.9 Measurement procedure

1) Calibrate the measurement equipment

   When the measurement equipment is turned ON, the calibration shall be performed with the proper calibration kit to measure within its specified measurement accuracy. The measurement system shall be warmed up sufficiently before starting the calibration.

2) Connect the test fixture

   Connect the connector of the test fixture to the coaxial connector of the previously calibrated measurement equipment.

3) Place the sample holder and measure the impedance Z_{sm}

   Place only the sample holder in the test fixture. Enter the measurement parameters, frequency range and oscillator output voltage level and other values, into the measurement equipment and measure the impedance Z_{sm} of the test fixture.

4) Place the NSS sample and measure the impedance Z_m

   Place the toroidal-shaped NSS sample with the sample holder in the test fixture coaxially and measure the impedance Z_m of the test fixture with a sample.

5) Calculate the relative permeability μ_r' and μ_r'' and uncertainties $u(\mu_r')$ and $u(\mu_r'')$

   Calculate the values of μ_r' and μ_r'' by using Formula (4) and Formula (5), respectively. The measurement uncertainties are also calculated by using Formula (6) to Formula (17).

5.1.10 Example of measurement results

The measurement results of μ_r' and μ_r'' for a NSS (sample A and B) are shown in Figure 6. The parameters of the sample are a = 3,00 mm, b = 7,00 mm and t = 0,20 mm (sample A) or 0,25 mm (sample B), and the oscillator output voltage level, about 0,1 V, is selected in order not to affect the results.

IECNORM.COM : Click to view the full PDF of IEC TR 63307:2020

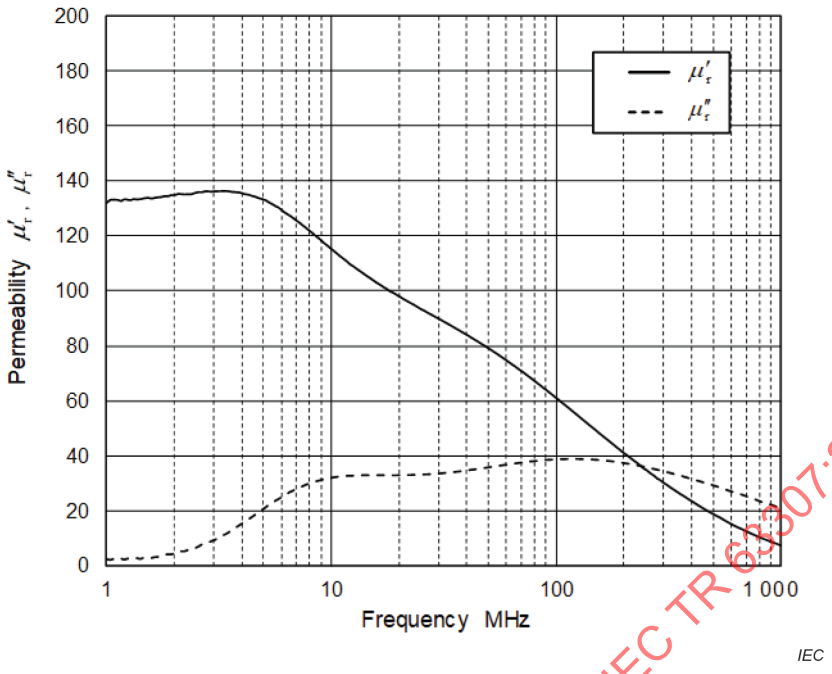

a) Sample A (t = 0,20mm)

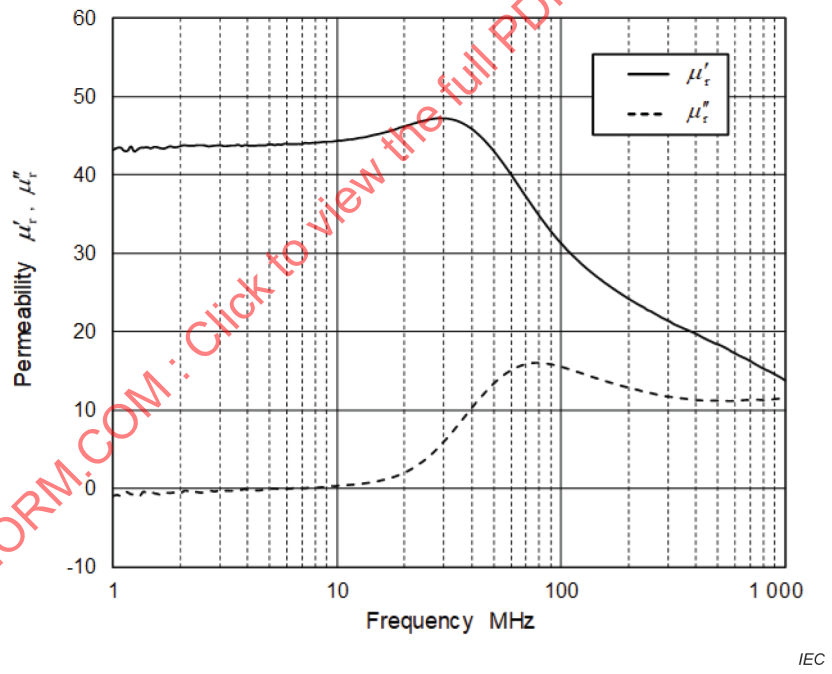

b) Sample B (t = 0,25mm)

Figure 6 – Measurement results of NSS samples

IECNORM.COM : Click to view the full PDF of IEC TR 63307:2020

5.1.11 Remarks

Subclause 5.1 provides some helpful information on measuring the magnetic properties of toroidal-shaped NSS samples using the inductance method.

1) The test sample should be made correctly in a toroidal shape and placed in the test fixture coaxially.
2) The measurement accuracy depends on the measured impedance values and gets worse in low frequencies because the measurement error increases with a decrease in the frequency.

3) The use of an impedance analyzer is recommended to measure the impedance because the impedance analyzer has the advantages of higher accuracy and wider impedance measurement range than a network analyzer.

4) The measurement results of μ_r' and μ_r'' may be obtained after measuring the impedance Z_{sm} and Z_m if the material analyzer is used. The measurement results of the impedance Z_{sm} and Z_m are not displayed because the software installed on the analyzer calculates and compensates the measurement results.

5) A sample with a low permeability or a thin thickness leads to measurement error. It is difficult to measure its permeability accurately due to the low impedance Z_{NSS} of a NSS sample. Stacking some samples is a better way to get the results needed.

6) When the permittivity of a NSS sample is high (more than about 10), current flows through the space between the NSS sample and the test fixture. This introduces an equivalent capacitance connected in parallel to the impedance of the sample Z_{NSS}. The resonance of this parallel LC circuit occurs at around 1 GHz or below and precise measurements will be difficult.

5.2 Nicolson Ross Weir method

5.2.1 Principle

The objective of this method is to evaluate the broadband properties of the complex relative permeability and permittivity of a noise suppression sheet by using a transmission line as coaxial line and waveguide. Measurement frequency ranges and accuracy depend on the test fixture and electromagnetic properties of a sample. This document describes a measurement method using a 7 mm coaxial transmission line. Complex relative permittivity and permeability are to be derived from the reflection and transmission coefficient of a sample inserted into a transmission line. Reflection and transmission coefficients are calculated from S-parameters S_{11} and S_{21} measured by a vector network analyzer. Figure 7 shows a schematic diagram of a test fixture with a sample and signal flow graph.

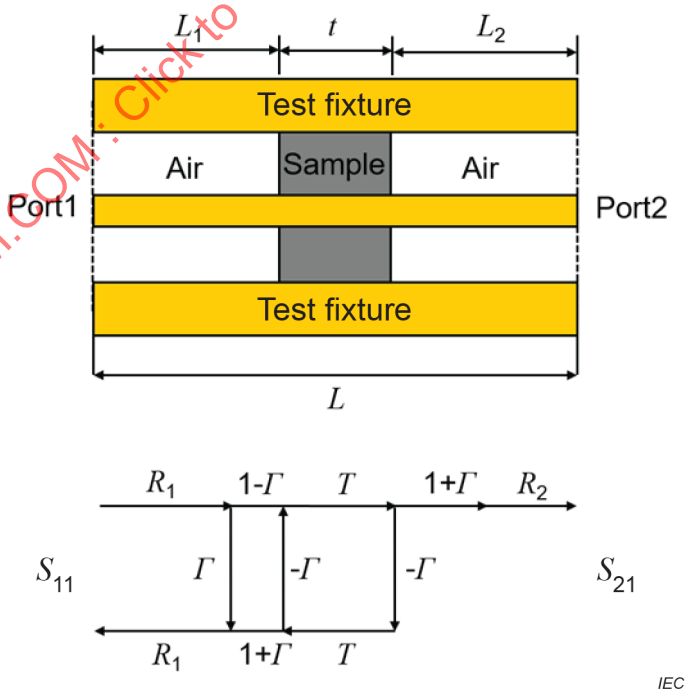

Figure 7 – Schematic diagram of a test fixture with a sample and signal flow graph

A signal is inserted from Port1. L and t are the length of a test fixture and sample L_1 and L_2 are the length from the respective reference plane to the sample faces.

IECNORM.COM : Click to view the full PDF of IEC TR 63307:2020

From a signal flow graph, the S-parameters on a transmission line with sample are given by

$$S_{11} = R_1^2 \frac{\Gamma\left(1-T^2\right)}{1-T^2\Gamma^2} \tag{18}$$

$$S_{21} = R_1 R_2 \frac{T\left(1-\Gamma^2\right)}{1-T^2\Gamma^2} \tag{19}$$

$$R_i = \exp\left(-\gamma_0 L_i\right) \ \left(i = 1,2\right) \tag{20}$$

where

Γ is the reflection coefficient at sample faces;

T is the transmission coefficient of a sample;

γ_0 is the propagation constant of air;

R_i is the transmission coefficient from the reference plane to the sample face at the respective ports.

Reflection coefficient Γ is defined by

$$\Gamma = \frac{Z_L - Z_0}{Z_L + Z_0} \tag{21}$$

$$Z_L = Z_0 \sqrt{\frac{\mu_r}{\varepsilon_r}} \tag{22}$$

where

Z_L and Z_0 are the characteristic impedance of a sample and air in the transmission line.

The transmission coefficient and propagation constant of a sample on a transmission line are given by

$$T = \exp(-\gamma d) \tag{23}$$

$$\gamma = \gamma_0 \sqrt{\mu_r \varepsilon_r} \tag{24}$$

where

γ is the propagation constant of a sample.

From Formula (18) to Formula (24), the complex relative permeability and permittivity of a sample are calculated by

IECNORM.COM : Click to view the full PDF of IEC TR 63307:2020

$$\mu_r = \left(\frac{1+\Gamma}{1-\Gamma}\right)\left(\frac{1}{\gamma_0 d}\ln\left(\frac{1}{T}\right)\right) \quad (25)$$

$$\varepsilon_r = \left(\frac{1-\Gamma}{1+\Gamma}\right)\left(\frac{1}{\gamma_0 d}\ln\left(\frac{1}{T}\right)\right) \quad (26)$$

It shall be noted that the calculated value is divergent at integral multiples of half wavelength in a sample.

5.2.2 Measurement frequency and accuracy

The objective of this method is to measure the broadband electromagnetic properties of a sample. Measurement frequency ranges and accuracy depend on the test fixture and electromagnetic properties of a test sample. The lower frequency is limited by the smallest measurable phase shift through a sample. The upper frequency limit is determined by the excitation of higher order modes that invalidates the dominant-mode transmission line. (In the case of a 7 mm coaxial transmission line, the frequency range can be set from 500 MHz to 18 GHz.)

5.2.3 Measurement parameters

The objective of this method is to measure the in-plane properties of the complex relative permeability and permittivity by using a transmission line. However, the magnetic and dielectric perpendicular properties of a noise suppression sheet are not measured. Figure 8 shows the cross section of coaxial line with NSS.

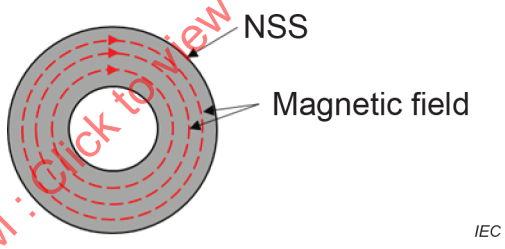

Figure 8 – Cross section of coaxial line with NSS

5.2.4 Test sample

Figure 9 shows the dimensions of a test sample. The dimensions of a sample depend on the test fixture. The sample shall fully fill the cross section of the transmission line. In the case of a 7 mm coaxial transmission line, the sample shall be fabricated in the shape of a toroidal ring. The preferable sample size is shown in Figure 9:

IECNORM.COM : Click to view the full PDF of IEC TR 63307:2020

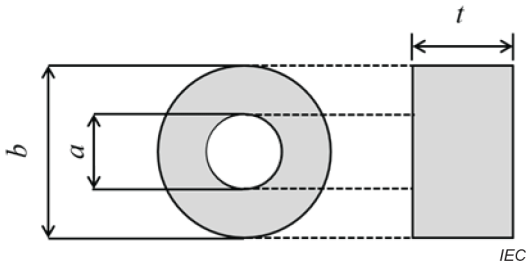

Inner diameter of test sample: a = 3,04 mm

Outer diameter of test sample: b = 7,00 mm

Length of test sample: t ≦ length of test fixture L.

Figure 9 – Dimensions of test sample

Each parameter should be measured with a precision of less than 1/100 mm using a micrometer. For measurement of a high complex relative permittivity material, a sample shall be manufactured more precisely because complex relative permittivity is influenced highly by the air gap between the sample and test fixture. The length of the sample should be such that the phase of S_{21} is less than half the wavelength.

5.2.5 Measurement environment

The test fixture and the samples shall be kept in a clean and dry state. The room temperature and the relative humidity shall preferably be 23 °C ± 5 °C and less than 60 %.

5.2.6 Measurement uncertainly

In the measurement uncertainties of ε'_r, ε''_r, μ'_r and μ''_r, $u(\varepsilon'_r)$, $u(\varepsilon''_r)$, $u(\mu'_r)$ and $u(\mu''_r)$, are estimated as the combined standard uncertainty and given respectively by

$$u(\mu'_r)^2 = \left(\frac{\partial \mu'_r}{\partial |S_{11}|}\right)^2 u(|S_{11}|)^2 + \left(\frac{\partial \mu'_r}{\partial \theta_{11}}\right)^2 u(\theta_{11})^2 + \left(\frac{\partial \mu'_r}{\partial |S_{21}|}\right)^2 u(|S_{21}|)^2 + \left(\frac{\partial \mu'_r}{\partial \theta_{21}}\right)^2 u(\theta_{21})^2 + \left(\frac{\partial \mu'_r}{\partial d}\right)^2 u(d)^2 + \left(\frac{\partial \mu'_r}{\partial G}\right)^2 u(G)^2 \quad (27)$$

$$u(\mu''_r)^2 = \left(\frac{\partial \mu''_r}{\partial |S_{11}|}\right)^2 u(|S_{11}|)^2 + \left(\frac{\partial \mu''_r}{\partial \theta_{11}}\right)^2 u(\theta_{11})^2 + \left(\frac{\partial \mu''_r}{\partial |S_{21}|}\right)^2 u(|S_{21}|)^2 + \left(\frac{\partial \mu''_r}{\partial \theta_{21}}\right)^2 u(\theta_{21})^2 + \left(\frac{\partial \mu''_r}{\partial d}\right)^2 u(d)^2 + \left(\frac{\partial \mu''_r}{\partial G}\right)^2 u(G)^2 \quad (28)$$

$$u(\varepsilon'_r)^2 = \left(\frac{\partial \varepsilon'_r}{\partial |S_{11}|}\right)^2 u(|S_{11}|)^2 + \left(\frac{\partial \varepsilon'_r}{\partial \theta_{11}}\right)^2 u(\theta_{11})^2 + \left(\frac{\partial \varepsilon'_r}{\partial |S_{21}|}\right)^2 u(|S_{21}|)^2 + \left(\frac{\partial \varepsilon'_r}{\partial \theta_{21}}\right)^2 u(\theta_{21})^2 + \left(\frac{\partial \varepsilon'_r}{\partial d}\right)^2 u(d)^2 + \left(\frac{\partial \varepsilon'_r}{\partial G}\right)^2 u(G)^2 \quad (29)$$

$$u(\varepsilon''_r)^2 = \left(\frac{\partial \varepsilon''_r}{\partial |S_{11}|}\right)^2 u(|S_{11}|)^2 + \left(\frac{\partial \varepsilon''_r}{\partial \theta_{11}}\right)^2 u(\theta_{11})^2 + \left(\frac{\partial \varepsilon''_r}{\partial |S_{21}|}\right)^2 u(|S_{21}|)^2 + \left(\frac{\partial \varepsilon''_r}{\partial \theta_{21}}\right)^2 u(\theta_{21})^2 + \left(\frac{\partial \varepsilon''_r}{\partial d}\right)^2 u(d)^2 + \left(\frac{\partial \varepsilon''_r}{\partial G}\right)^2 u(G)^2 \quad (30)$$

where

θ_{11} and θ_{21} are the phases of the S-parameter;

G is the air gap between the sample and test fixture.

IECNORM.COM : Click to view the full PDF of IEC TR 63307:2020

The uncertainties used for the S-parameters depend on the vector network analyzer used for the measurements. This type of uncertainty analysis assumes that changes in independent variables are sufficiently small so that a Taylor series expansion is valid. There are many other uncertainty sources of lesser magnitude such as repeatability of connections and torqueing of connectors. Estimates for these uncertainties could be added to the uncertainty budget sheet.

5.2.7 Measurement system

Figure 10 shows a schematic diagram of the equipment system for the measurement. For the measurement of the S-parameter, the vector network analyzer is connected to a test fixture.

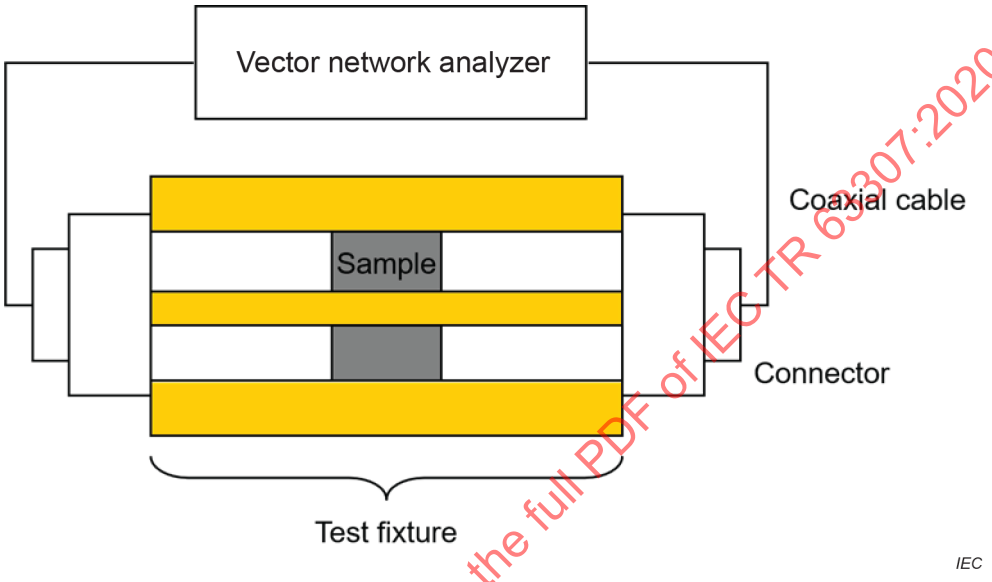

Figure 10 – Schematic diagram of equipment system for measurement

5.2.8 Test fixture

Various transmission lines can be used as a test fixture. For example, Figure 11 shows a specification for a test fixture in the case of a 7 mm coaxial transmission line. The test fixture consists of an inner conductor and outer conductor. The length of the test fixture shall be longer than or equal to the length of the sample. A test fixture shall be connected to connectors which are connected to the vector network analyzer.

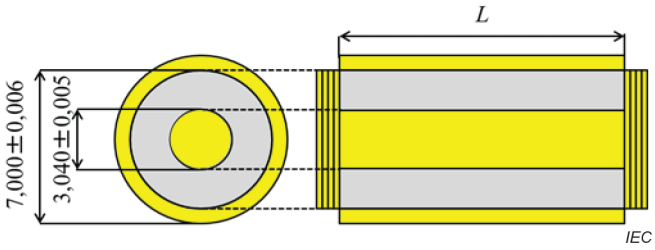

Figure 11 – Specification for test fixture of a 7 mm coaxial transmission line

5.2.9 Measurement procedure

1) When the network analyzer is turned ON, the calibration shall be performed with the proper calibration kit to measure within its specified measurement accuracy. The measurement system shall be warmed up sufficiently before starting the calibration.
2) The sample is inserted into the test fixture. Connect the connector of the test fixture to the connector of the previously calibrated network analyzer.

IECNORM.COM : Click to view the full PDF of IEC TR 63307:2020

3) The S-parameters $S_{11}$and S_{21} of the test fixture with a sample are measured by using the network analyzer.

4) The values of the complex permeability and permittivity are calculated by using Formula (18), Formula (19), Formula (25) and Formula (26), respectively. The measurement uncertainties are estimated by using Formula (27) to Formula (30).

5.2.10 Example of measurement results

Figure 12 shows the measurement results of ε'_r, ε''_r, μ'_r and μ''_r for a noise suppression sheet with a thickness of 0,5 mm. A 7 mm coaxial transmission line is used for the measurement.

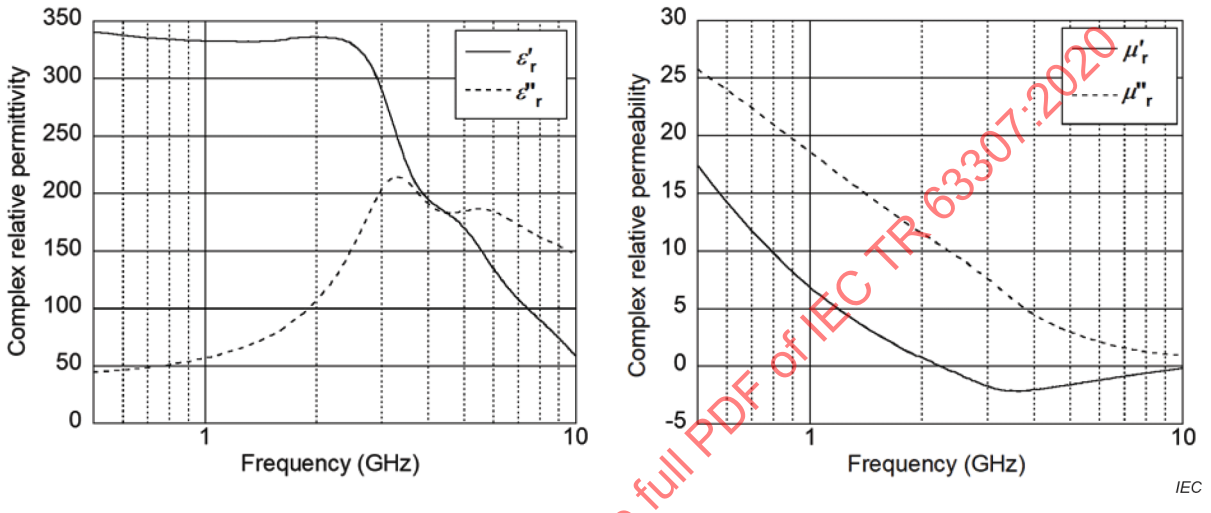

(a) Sample A

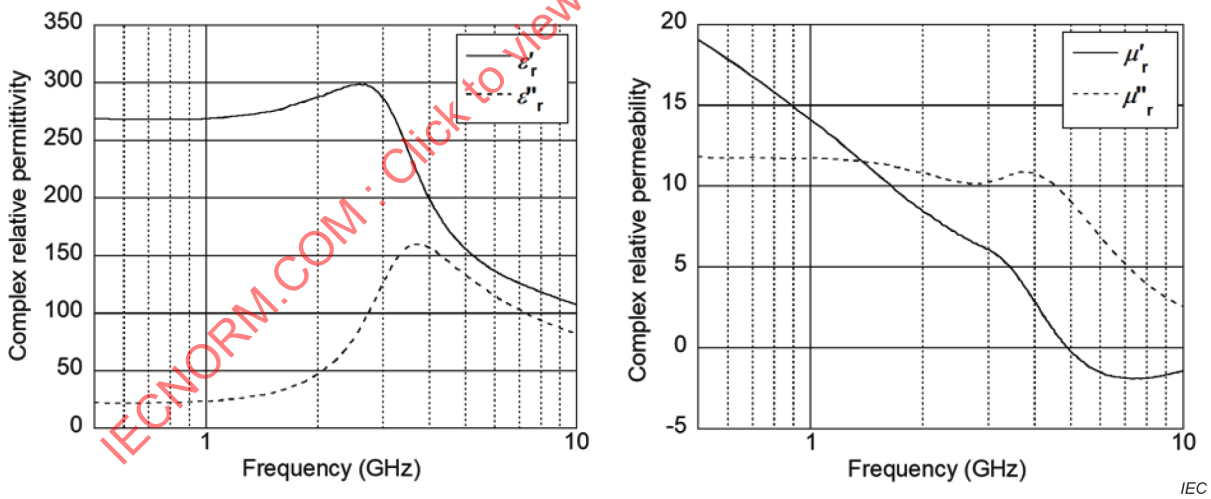

(b) Sample B

Figure 12 – Measurement results of noise suppression sheet

IECNORM.COM : Click to view the full PDF of IEC TR 63307:2020

5.2.11 Remarks

Subclause 5.2 provides some helpful information on measuring the complex relative permittivity and permeability using the Nicolson Ross Weir method.

1) Coaxial transmission lines cover a broad frequency range, but a toroid-shaped sample is more difficult to manufacture. It shall be noted that complex relative permittivity is very much influenced by the air gap between a sample and test fixture.

2) When measuring a sample with a thickness of more than half the wavelength using the Nicolson Ross Weir model, discontinuities can appear in the trace.

3) A guided jig made of low dielectric and loss tangent material such as styrene foam is effective to hold a sample inside the test fixture. When using the guided jig, measure a standard sample with known material constants such as polytetrafluoroethylene (PTFE) with the guided jig and confirm that the guided jig does not affect the measurement results.

4) It shall be noted that the complex relative permittivity of NSS can be affected by self-resonance of the sample or test fixture. Another size of sample or test fixture should be measured to confirm the effect of the self-resonance.

5.3 Short-circuited microstrip line method

5.3.1 Principle

The measurement method evaluates the in-plane complex relative permeability of a rectangular shape sample of a noise suppression sheet (NSS) using a short circuit microstrip line (MSL) jig. The rectangular shaped NSS sample is placed at the MSL short-circuited end. In this measurement method, two S_{11} values of the MSL jig with sample are measured when an external static strong magnetic field is applied to the sample and when it is not applied to the sample, respectively; the permeability is then calculated. This method is denoted as a field method in this measurement.

The reference plane is denoted on the source side plane of the rectangular sample. The lumped element parallel LC equivalent circuits are assumed as shown in Figure 13. The S_{11} parameter is measured and analyzed to derive the permeability of the sample based on the lumped element approximation. Figure 13a) and Figure 13 b) are the equivalent circuits for the blank test fixture and for the sample loaded test fixture, respectively. Figure 13 c) shows the equivalent circuit for the test fixture with sample under the external static strong magnetic field when the (as-measured) complex relative permeability of the sample is assumed to be 1. Y, C, L, and G are the input admittance, capacitance, inductance, and conductance for the equivalent circuit in the MSL jig, respectively; the subscripts SHT, SMP, and SOM indicate the “short”, “sample” and “sample on magnet”; the subscripts "o" and "s" indicate the blank state (without sample) in the MSL jig and the presence of a sample in the MSL jig; ε'_r and ε''_r are the real and imaginary parts of complex relative permittivity; μ'_r and μ''_r are the real and imaginary parts of complex relative permeability; and ω (= $2\pi f$) is the measurement frequency. The observed permeability of the sample essentially includes the demagnetization effect that originated in the rectangular shape of the sample. Consequently, the as-measured complex relative permeability should be corrected by the demagnetization factor N and coupling constant η. The details for the calculation are described in Annex B.

IECNORM.COM : Click to view the full PDF of IEC TR 63307:2020

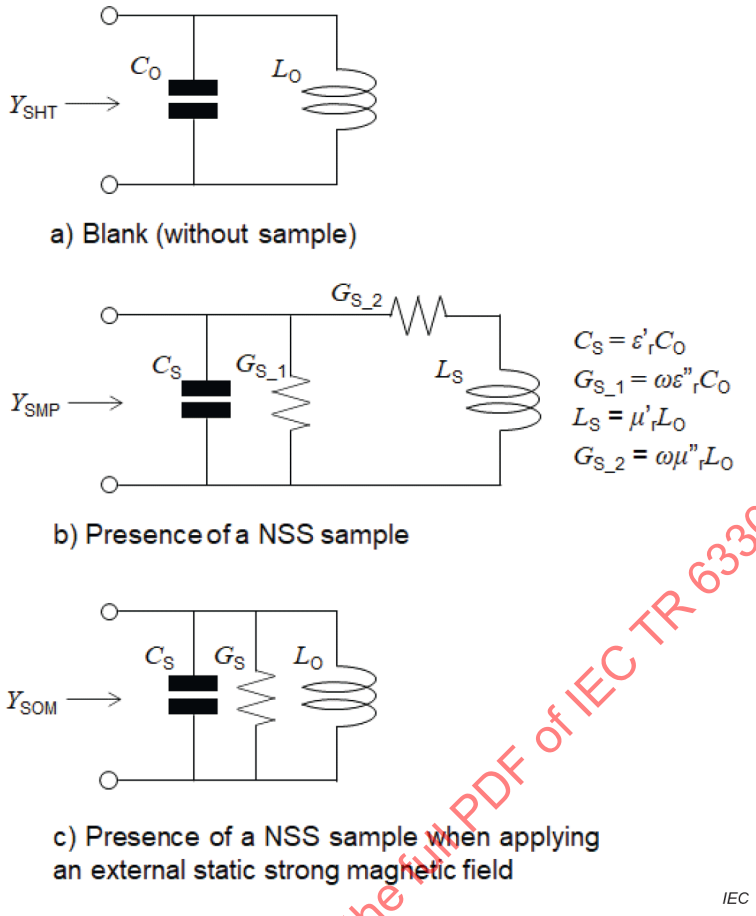

Figure 13 – Equivalent circuits for the MSL

5.3.2 Measurement frequency and accuracy

The objective of this method is to evaluate NSS samples and is applicable for the measurements under the following conditions:

frequency: 10 MHz ≤ f ≤ 10 GHz

relative permeability: $\mu'_r \leq 1\,000$, $0 \leq \mu''_r \leq 1\,000$

accuracy (repetitive): value error ± 5 %

5.3.3 Measurement parameters

The in-plane complex relative permeability $\mu'_r - j\mu''_r$ of the NSS sample is measured.

5.3.4 Test sample

A rectangular shape is prepared from the NSS sample as shown in Figure 14.

IECNORM.COM : Click to view the full PDF of IEC TR 63307:2020

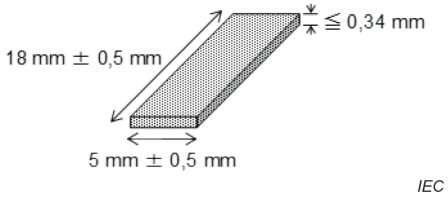

Long axis: 18 mm ± 0,5 mm

Short axis: 5 mm ± 0,1 mm

Thickness: $t \leq 0{,}34$ mm

Figure 14 – Rectangular shape of NSS sample

It is necessary that the rectangular shape sample be uniform (homogeneous) without cracks, cuts, and rupture surface irregularities. The accurate value of the permeability of the sample depends on its accurate thickness.

5.3.5 Measurement environment

The fixture and the samples shall be kept in a clean and dry state. The room temperature and the relative humidity shall preferably be 23 °C ± 5 °C and less than 60 %, respectively. It is desirable to secure a place where the temperature and the humidity are constant, or in a space where equipment (including the jig) and cables are deployed in a housing with constant temperature and humidity. Introduced variables such as temperature changes or jig detachment because of handling should be minimized.

5.3.6 Measurement system

The apparatus of the permeability measurement system is shown in Figure 15. The MSL jig is connected to a vector network analyzer (VNA) via a coaxial cable, and the VNA communicates through a personal computer (PC). The electric signal from the VNA is analyzed by the PC installed software for permeability. When the permeability of samples is measured, a permanent magnet is used.

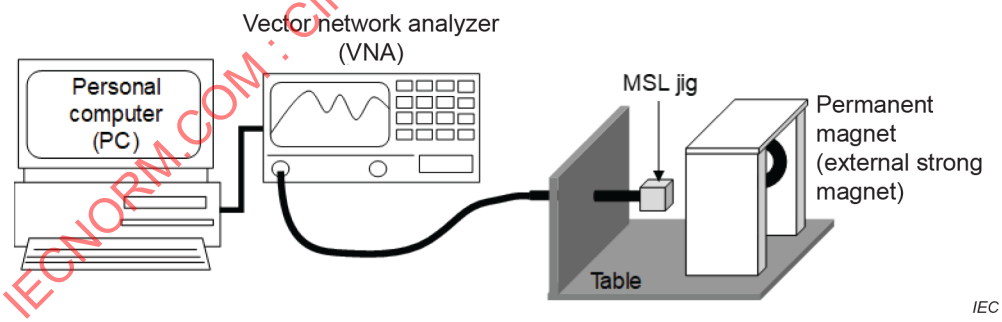

Figure 15 – Measurement system

5.3.7 Test fixture (MSL jig)

Figure 16 shows a short-circuited test fixture (MSL jig) and sample installation. The MSL jig consists of a short-circuited microstrip line, and another end of the microstrip line is connected to the SMA connector. The rectangular shape sample is uniformly and tightly placed at the corner of the short end. When a gap between the ground conductor of the short-circuited end and the sample is too large, the correct result cannot be obtained. A table that supports the MSL jig and a permanent magnet are also prepared (see Figure 16).

IECNORM.COM : Click to view the full PDF of IEC TR 63307:2020

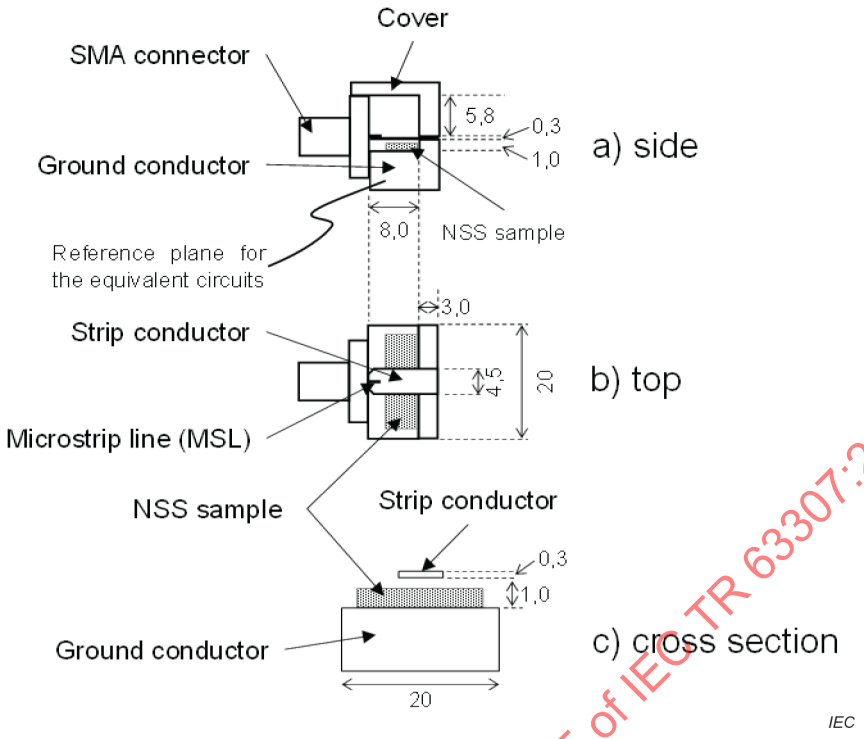

Figure 16 – Short-circuited microstrip line test fixture (MSL jig)

5.3.8 Measurement procedure

1) Set up the VNA, frequency range (10 MHz ≤ f ≤ 10 GHz). For example: VNA set up parameters, measurement points: 401, IF bandwidth: 1 kHz, power: −17 dBm, average: 5.
2) Set the measurement parameter of VNA to S_{11}.
3) Connect a coaxial cable and the VNA.
4) Calibrate the connected coaxial cable using calibration kits (open, short, and load).
5) Connect the coaxial cable end and the test fixture (MSL jig).
6) Measure S_{11} of the blank state of the MSL jig and store as S_{11_SHT}.
7) Measure S_{11} of the NSS rectangular shape sample placed in the MSL jig by applying an external static strong magnetic field and store as S_{11_SOM}.
8) Measure S_{11} of the NSS rectangular shape sample placed in the test fixture by removing the external static strong magnetic field and store as S_{11_SMP}.

5.3.9 Results (example)

Figure 17 shows the measurement and corrected results of the complex relative permeability for a NSS sample C with 0,236 mm thickness. The measurement results are corrected by demagnetization factor N and coupling coefficient η.

IECNORM.COM : Click to view the full PDF of IEC TR 63307:2020

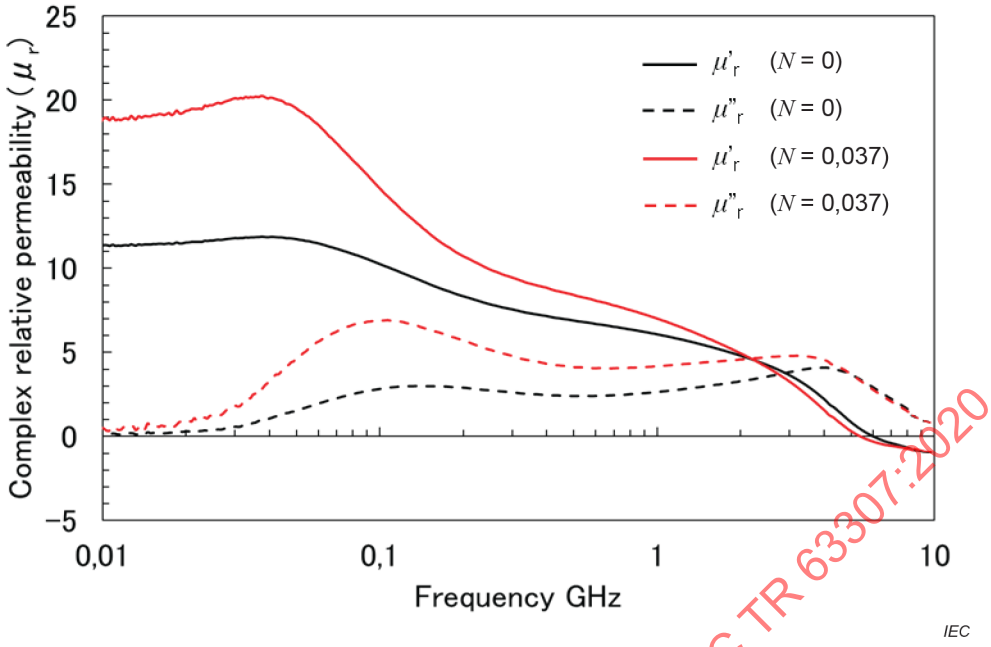

Figure 17 – Complex relative permeability of a NSS sample C with 0,236 mm thickness, as measured at N = 0 (and η = 0,135 2) and corrected by demagnetization factor N = 0,037 (and η = 0,135 2)

5.3.10 Remarks

1) This method belongs to the field method which compares S_{11} parameters with the strong static magnetic field and without it, with the result that the influence of permittivity on the permeability measurement is small.
2) The saturated magnetization of NSS samples depends on the magnetic metal materials in the NSS. The magnetic metal materials sometimes show ferromagnetic resonance without saturating magnetization at 5 000 Oe, with the result that the imaginary part (μ''_r) of the permeability becomes a negative value at around 10 GHz. In this case, to observe reasonable results, further strong magnetic field will be required to saturate the NSS sample.
3) The magnetization of the NSS (or magnetic) sample is necessary to saturate more than 90 % at the applied strong static magnetic field (approximately 5 000 Oe).

5.4 Short-circuited coaxial line method

5.4.1 Principle

The measurement method evaluates the in-plane complex relative permeability μ_r of a NSS sample with a toroidal shape using a short circuit coaxial line (denoted coax) jig. In this method, the lumped element approximation is employed for the data analysis. This method is called a "remove" method, in which two S_{11} values corresponding to the blank (without sample) and to the NSS sample are compared. The demagnetization in toroidal shape samples is not considered (i.e., zero) because the sample with shape is endless and fully occupied for the magnetic material.

IECNORM.COM : Click to view the full PDF of IEC TR 63307:2020

In general, the permittivity of the NSS sample affects the permeability of the sample. The influence of the permittivity on the permeability becomes pronounced when increasing the thickness of the sample. Experimentally in this method, when the sample thickness is 0,3 mm or less, the influence can be almost ignored. In contrast, when it is more than 0,3 mm, the permittivity shall be corrected by the permeability. The complex relative permittivity ε_r of the NSS sample can be measured by the open-circuited coaxial line as indicated in Annex C, and then the permeability can be corrected by the obtained permittivity. However, if the sample thickness exceeds the above acceptable value, the permeability cannot be corrected appropriately. This is because the lumped element approximation in this method cannot be described. To describe the lumped element approximation, the phase shift βt is calculated and required to be less than 0,8 rad, where β is the phase constant (= $(2\pi(\varepsilon_r\mu_r)^{1/2}f)/c$), t is the sample thickness, f is the frequency, and c is the light speed in a vacuum. The ε_r is measured by the open-circuited coaxial line (see Annex C). That is, if the βt is less than 0,8 rad in the measurement frequency band, the permeability is appropriately corrected by the obtained permittivity.

The reference plane for the measurement is the source side plane of toroidal sample. The lumped element parallel LC equivalent circuit is assumed as shown in Figure 18. Figure 18a) and Figure 18b) are the equivalent circuits for the blank state (without sample) and the presence of the sample in the coax jig, respectively. Y, C, L, and G are the input admittance, capacitance, inductance, and conductance for the equivalent circuit in the coax jig; the subscripts SHT and SMP indicate the "short" and "sample"; subscripts "o" and "s" indicate the blank state and presence of sample in the coax jig; ε'_r and ε''_r are the real and imaginary parts of the complex relative permittivity; μ'_r and μ''_r are the real and imaginary parts of the complex relative permeability; and ω (= $2\pi f$) is the measurement frequency. The details for the calculation are described in Annex C.

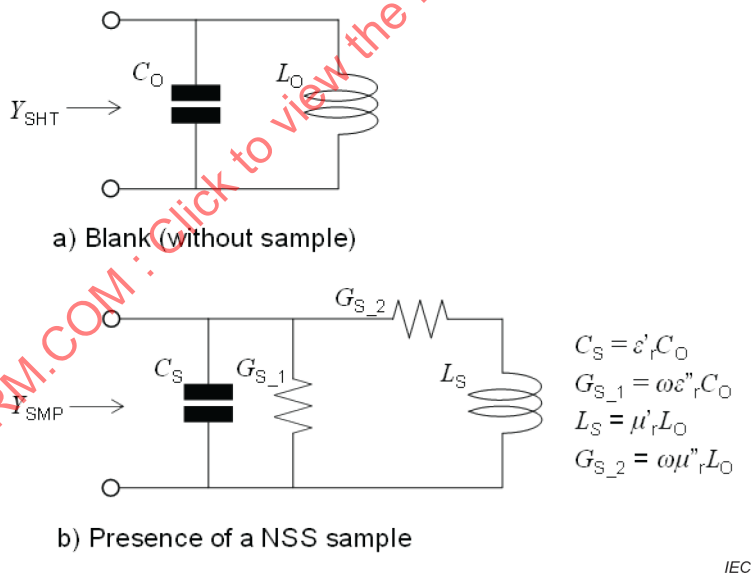

Figure 18 – Equivalent circuits for the coax jig

5.4.2 Measurement frequency and accuracy

The objective of this method is to evaluate NSS samples and is applicable for the measurements under the following conditions:

frequency: 1 MHz ≤ f ≤ 10 GHz

relative permeability: μ'_r ≤ 1 000, 0 ≤ μ''_r ≤ 1 000

accuracy (repetitive): value error ± 5 %

IECNORM.COM : Click to view the full PDF of IEC TR 63307:2020

The lowest frequency can be expanded with a thicker sample. If the permittivity effect is negligible with a thinner sample, the highest frequency could be expanded up to 18 GHz.

5.4.3 Measurement parameters

The in-plane complex relative permeability $\mu'_r - j\mu''_r$ of NSS samples is measured.

5.4.4 Test sample

A toroidal shape prepared from a NSS sample is shown in Figure 19.

Inner diameter: $3\,^{+0,05}_{0}$ mm

Outer diameter: $7^{0}_{-0,05}$ mm

Thickness: To be determined to describe the lumped element approximation, depending on the maximum frequency (typically, $t \leq 0{,}3$ mm).

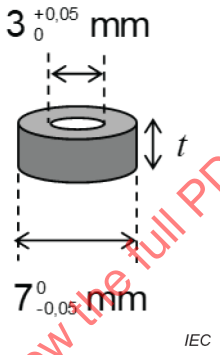

Figure 19 – Toroidal shape of NSS sample

5.4.5 Measurement environments

The fixture and the samples shall be kept in a clean and dry state. The room temperature and the relative humidity shall preferably be 23 °C ± 5 °C and less than 60 %, respectively. The temperature slightly affects the measurement results. Especially, the effect is provably large below 1 GHz. Therefore, it is desirable to secure the place where the temperature and the humidity are constant, or the space where equipment (including the jig) and cables are deployed in a housing with constant temperature and humidity. Introduced variables such as temperature changes or jig detachment because of handling should be minimized.

5.4.6 Measurement system

The apparatus of the permeability measurement system is shown in Figure 20. The coax jig is connected to a vector network analyzer (VNA) via a coaxial cable, and the VNA communicates through a personal computer (PC). The electric signal from the VNA is analyzed by software on the PC to determine permeability.

IECNORM.COM : Click to view the full PDF of IEC TR 63307:2020

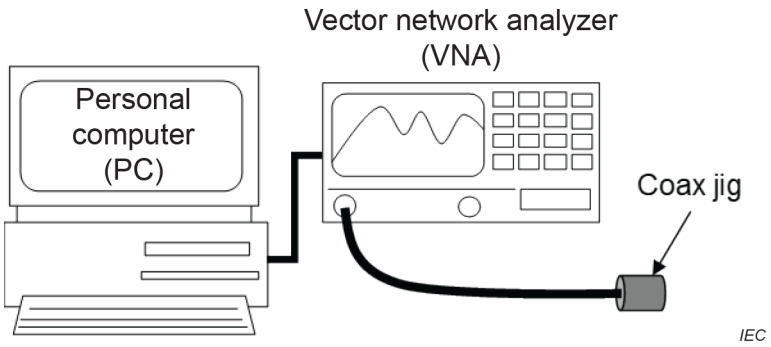

Figure 20 – Measurement system

5.4.7 Test fixture (coax jig)

Figure 21 shows the cross-sectional diagram of the practical test fixture coax jig in detail. The coax jig is connected to an APC-7 adapter and then the other side of the APC-7 adapter is connected to the SMA connector. The toroidal shape sample having the same diameter dimensions as APC-7 is tightly inserted at the end of the short-circuited coaxial line. Measure S_{11_SHT} and S_{11_SMP} corresponding to the blank and to the loaded test fixture, respectively.

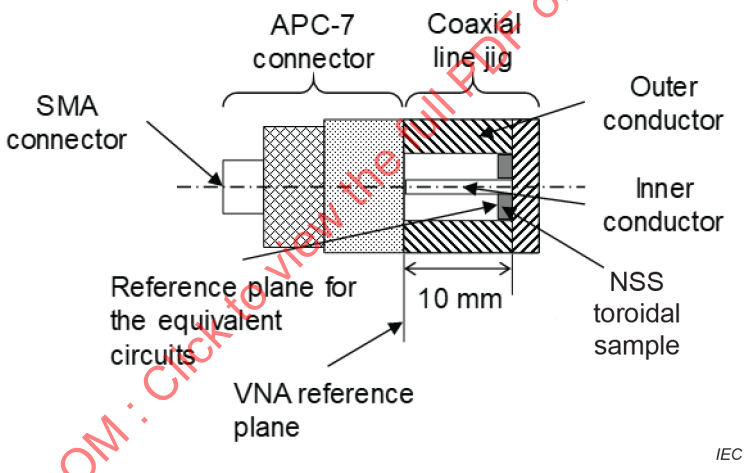

Figure 21 – Short-circuited coaxial line test fixture (coax jig)

5.4.8 Measurement procedure

1) Set up the VNA, frequency range (1 MHz ≤ f ≤ 10 GHz). For example, VNA set up parameters, measurement points: 401, IF bandwidth: 1 kHz, power: −17 dBm, average: 5.
2) Set the measurement parameter of VNA to S_{11}.
3) Connect a coaxial cable and VNA.
4) Calibrate the connected coaxial cable including APC-7 using calibration kits (open, short, and load).
5) Connect the coaxial cable end (APC-7) and the test fixture (coax jig).
6) Measure S_{11} of the blank state of the coax jig and store as S_{11_SHT}.
7) Measure S_{11} of the NSS toroidal shape sample placed in the coax jig and store as S_{11_SMP}.

IECNORM.COM : Click to view the full PDF of IEC TR 63307:2020

5.4.9 Results (example)

Figure 22 and Figure 23 show the measurement corrected results of the complex relative permeability for NSS sample A with 0,29 mm thickness and sample B with 0,25 mm thickness. The measurement results (as measured μ'_r and μ''_r) are corrected by the permittivity. The corrected results are almost the same as the measured results. In these samples with thickness, the permittivity almost does not affect the complex permeability. In the low frequency region between 0,001 GHz and 0,005 GHz, the measurement spectra (μ'_r and μ''_r) are distorted and/or noisy. The distortion degree depends on the sample and the size precision (dimension accuracy) of the toroidal shape (see 5.4.4). However, this region approaches the measurement limit for this method using the coax jig.

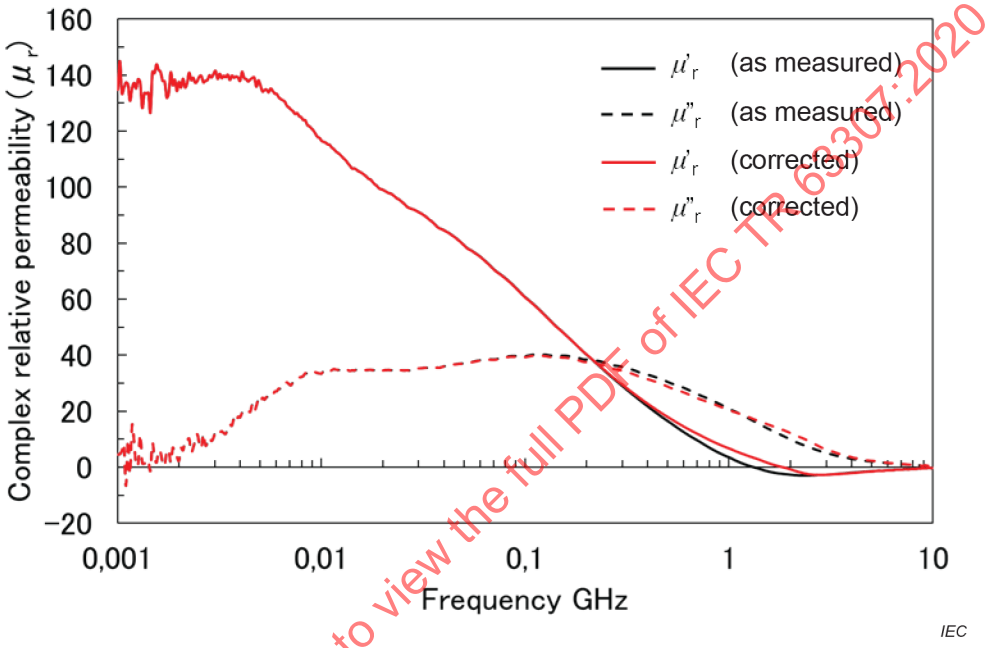

Figure 22 – Complex relative permeability of a NSS sample A with 0,29 mm thickness, as measured and corrected by the permittivity

IECNORM.COM : Click to view the full PDF of IEC TR 63307:2020

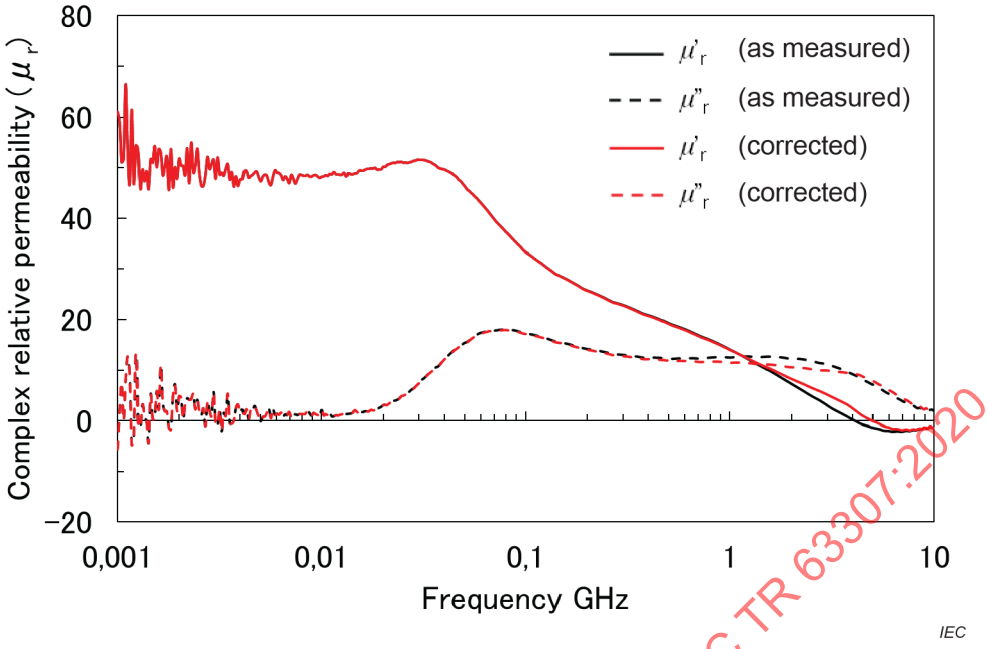

Figure 23 – Complex relative permeability of a NSS sample B with 0,25 mm thickness, as measured and corrected by the effective permittivity

5.4.10 Remarks

The complex relative permeability of samples is measured. As mentioned before, the measurement spectra are distorted and/or noisy in the low frequency region. This distortion degree depends on the sample and the size precision of the toroidal shape. This suggests the measurement limit for this method. The influence of the permittivity on the permeability for the sample is also investigated (see Annex C). In fact, when a sample with a thickness ≤ 0,3 mm is measured, the effect is very small at the measurement frequency region less than 1 GHz. A slight effect is seen around 1 GHz or more. This effect is smaller for thinner NSS samples. An experimental confirmation is necessary for the upper limit thickness of NSS below which the permittivity does not affect the permeability.

5.5 Shielded loop coil method

5.5.1 Measurement principle

5.5.1.1 General description

The shielded loop coil is a one-turn coil that will enclose the NSS in the coil window and pick up flux voltage as a signal from the NSS driven by an external AC magnetic field H_{AC}. The source of the AC magnetic field is a Transverse Electromagnetic (TEM) cell that encloses the shielded loop and the NSS near the surface of the ground conductor. By applying an RF signal to the TEM cell, the AC magnetic field H_{AC} is generated to the right angle of the strip conductor. The magnetic relative permeability is derived from the change in the transmission parameter S_{21} from the TEM cell to the shielded loop in the state where the ferromagnetic nature of the NSS is killed by applying a strong DC magnetic field, and in the state where no DC magnetic field is applied.

5.5.1.2 Shielded loop coil

Figure 24 shows the structure of the shielded loop coil. The shielded loop coil consists of three metal layers that allow protection of unnecessary voltage injection from the stray AC electric field component E_{AC} around the coil. Accordingly the shielded loop coil is sensitive only to the magnetic component out of the electromagnetic signal.

IECNORM.COM : Click to view the full PDF of IEC TR 63307:2020

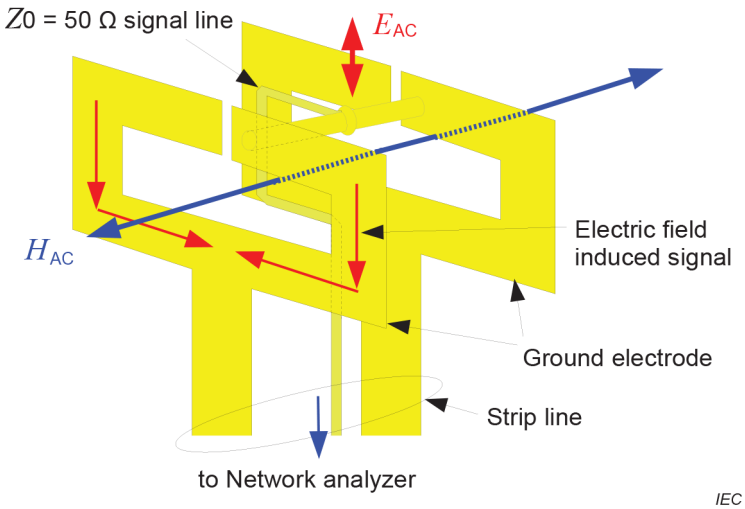

Figure 24 – Structure of shielded loop coil

Figure 25a) explains the shielded loop coil and NSS sample arrangement. The NSS is subjected to a uniform AC magnetic field H_{AC} in the direction parallel to the NSS sample surface and perpendicularly to the coil plane. Accordingly the shielded loop coil will measure complex relative permeability along the in-plane direction of the NSS.

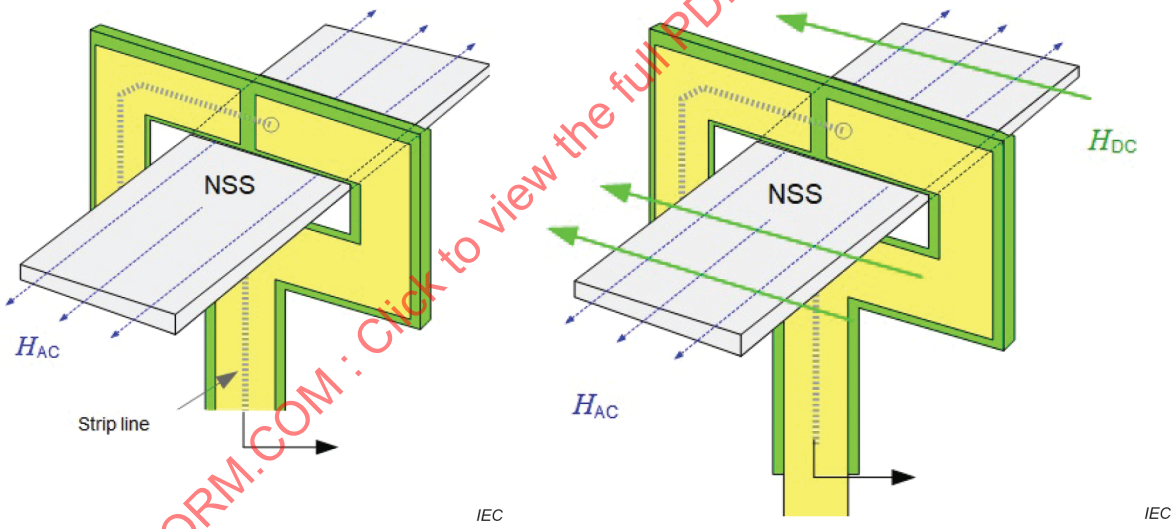

a) Direction of H_{AC} (main measurement)

b) Direction of H_{AC} and H_{DC} (reference measurement)

Figure 25 – Shielded loop coil and NSS sample arrangement

IECNORM.COM : Click to view the full PDF of IEC TR 63307:2020

5.5.1.3 AC and DC magnetic field application

Figure 26 shows the whole structure of the measuring unit of the equipment. The shielded loop coil and NSS sample are placed near the surface of the ground conductor of an RF cavity having an open TEM cell structure on the side. A terminal of the TEM cell is connected to Port 1 of a vector network analyzer that generates the RF signal. The other terminal of the TEM cell is connected to a 50 Ω load resistor.

Accordingly a traveling electromagnetic field is generated in the RF cavity, and the magnetic component H_{AC} of the field is used to measure the complex relative permeability. The electric component E_{AC} of the field will not disturb the relative permeability measurement thanks to the physical nature of the shielded loop coil to suppress electric-field induced voltage, as illustrated

in Figure 24. The TEM cell is matched to the characteristic impedance of Z_0 = 50 Ω and applies a uniform magnetic field to the NSS over the entire measurement frequency range. The reflection signal S_{11} from the TEM cell is negligible because the TEM cell is matched to Z_0 = 50 Ω.

For calibration purposes, the DC magnetic field H_{DC} is applied to the in-plane direction at the right angle to the AC magnetic field H_{AC}, as illustrated in Figure 25b). A DC magnetic field generator (e.g. solenoid coil) applies the DC magnetic field H_{DC} from outside the TEM cell, as shown in Figure 26.

Note that the relative directions of H_{AC}, H_{DC} and E_{AC} are the same throughout Figure 24 to Figure 26, with respect to the shielded loop coil and NSS sample directions.

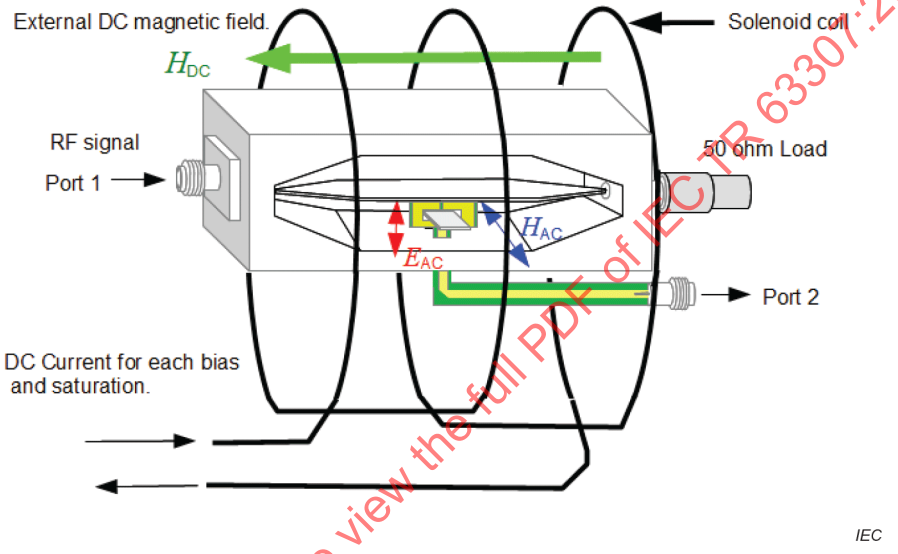

Figure 26 – Whole structure of the measuring unit of the equipment

IECNORM.COM : Click to view the full PDF of IEC TR 63307:2020

5.5.1.4 Theory of complex relative permeability measurement

5.5.1.4.1 General

The complex relative permeability $\mu_r = \mu'_r - \mu''_r$ can be obtained in principle from the frequency dependent transmission coefficient S_{21} of the S-parameter as it corresponds to the time rate of the magnetic flux linkage through the window of the shielded loop coil (flux voltage). The magnetic flux consists of air core flux and ferromagnetic flux. Two types of measurement are performed in order to separate the two kinds of fluxes.

5.5.1.4.2 Reference measurement

Transmission coefficient S_{21S} is measured under the application of the frequency dependent AC magnetic field H_{AC} where the NSS is saturated with a strong external DC magnetic field $H_{DC} = H_{sat}$. This measurement extracts the signal from the air core flux and the stray signal from the dielectric and resistive materials associated with the measurement unit. Reflection coefficient S_{22S} of the shielded loop coil is also measured to calibrate the impedance of the coil with the NSS sample having a non-magnetic nature.

5.5.1.4.3 Main measurement

Transmission coefficient S_{21N} is measured under the application of the frequency dependent AC magnetic field H_{AC} where H_{DC} = 0. This measurement extracts the ferromagnetic signal of

interest and all signals given by the reference measurement. Therefore the difference between the main and reference measurements corresponds to the ferromagnetic signal of interest. Reflection coefficient S_{22N} of the shielded loop coil is also measured to calibrate the impedance of the coil with the NSS sample having a ferromagnetic nature.

Accordingly, the complex relative permeability, $\mu_r = \mu'_r - \mu''_r$ is given by the Formula (31).

$$\mu_r = \frac{S_c}{S_m}\left[\frac{S_{21N}}{S_{21S}}\cdot\frac{1 - S_{22S}}{1 - S_{22N}} - 1\right] + 1 \tag{31}$$

where

S_m is the cross-sectional area of the NSS sample placed at the centre of the shielded loop coil;

S_c is the cross-sectional area of the effective aperture window of shielded loop coil;

S_{21S} is the transmission coefficient S_{21} measured when the NSS sample is saturated by an external DC magnetic field $H_{DC} = H_{sat}$ (for example, using a solenoid coil);

S_{21N} is the transmission coefficient S_{21} measured when the external DC magnetic field is removed ($H_{DC} = 0$) and the NSS sample is unsaturated;

S_{22S} is the reflection coefficient S_{22} measured when the NSS sample is saturated by a strong external DC magnetic field $H_{DC} = H_{sat}$ (for example, using a solenoid coil);

S_{22N} is the reflection coefficient S_{22} measured when the external DC magnetic field is removed ($H_{DC} = 0$) and the NSS sample is unsaturated.

5.5.1.4.4 RF calibration

Accuracy of measurement can be improved by taking account of the self-resonance nature of the shielded loop coil especially when the frequency approaches the self-resonance frequency of the shielded loop coil. Measure the impedance of the shielded loop coil without NSS to obtain inductance L_0, capacitance C_0 and self-resonance angular frequency ω_0. The relation $\omega_{02} = 1 / L_0 C_0$ stands. Then the complex relative permeability is calculated using Formula (32).

$$\mu_r = \frac{S_c}{S_m}\left[\frac{S_{21N}}{S_{21S}}\cdot\frac{1 - S_{22S} - S_{21S}}{1 - S_{22N} - S_{21N}}\cdot\frac{1}{1+\left[\frac{1 - S_{22S} - S_{21S}}{1 - S_{22N} - S_{21N}} - 1\right]\frac{\omega^2}{\omega_0^2}} - 1\right] + 1 \tag{32}$$

where,

ω is the angular frequency $\omega = 2\pi f$;

ω_0 it the self-resonance angular frequency of shielded loop coil: ${\omega_0}^2 = 1 / L_0 C_0$;

L_0 is the inductance of the shielded loop coil;

C_0 is the capacitance of the shielded loop coil.

5.5.1.4.5 Magnetic calibration (absolute value calibration)

Following the RF calibration in 5.5.1.4.4, 5.5.1.4.5 describes the magnetic calibration (absolute value calibration) of the complex relative permeability of the NSS sample. This calibration allows magnetic leakage flux compensation that returns outside the NSS but inside the shielded loop

IECNORM.COM : Click to view the full PDF of IEC TR 63307:2020

coil window. A frequency-independent scalar calibration constant is derived and used in the calibration procedure.

Figure 27 shows the DC magnetization curve of a NSS sample. Magnetization M is saturated to the saturation magnetic moment M_s when the DC magnetic field H_{DC} becomes more than the anisotropy field H_k. There is a known ferromagnetic theory applicable to the magnetic saturation range ($H_{DC} \gg H_k$).

$$M_s = (H_k + H_{DC})\,\mu_0\,\mu_r \tag{33}$$

Based on Formula (33), the absolute value of the complex relative permeability can be calibrated by the following procedure.

1) Measure relative permeability using Formula (32) with DC magnetic field H_{biasi} (i = 1,2,3⋯, H_{DC} = H_{biasi} << H_{sat}), instead of H_{DC} = 0. H_{biasi} is usually set several times the H_k. Thus obtained, the relative real and imaginary part relative permeability are called μ'_{rob} and μ''_{rob}, respectively, in 5.5.1.4.5.
2) Calculate the product of the real part of complex relative permeability μ'_{rob} and (H_{biasi} + H_k), namely (H_{biasi} + H_k)·μ'_{rob}. This product should be equal to the saturated magnetization M_s as the H_{biasi} strengthens because of Formula (33). However, the product will be less than the M_s however strong the H_{biasi} can be, because of the leakage flux that returns outside the NSS but inside the shielded loop coil window.
3) Draw the M_s versus the 1/(H_{biasi} + H_k) plot as shown in Figure 28.
4) Extrapolate the plot to cross the vertical axis to find M'_s as the estimate of the saturated magnetization when an infinitely high H_{bias} is applied.
5) Find the calibration coefficient M_s / M'_s. The calibrated complex relative permeability is obtained by multiplying this calibration coefficient M_s / M'_s to the real part μ'_{rob} and imaginary part μ''_{rob} of the complex relative permeability.

$$\mu_r = (M_s / M'_s) \cdot (\mu'_{rob} - j\mu''_{rob}) \tag{34}$$

IECNORM.COM : Click to view the full PDF of IEC TR 63307:2020

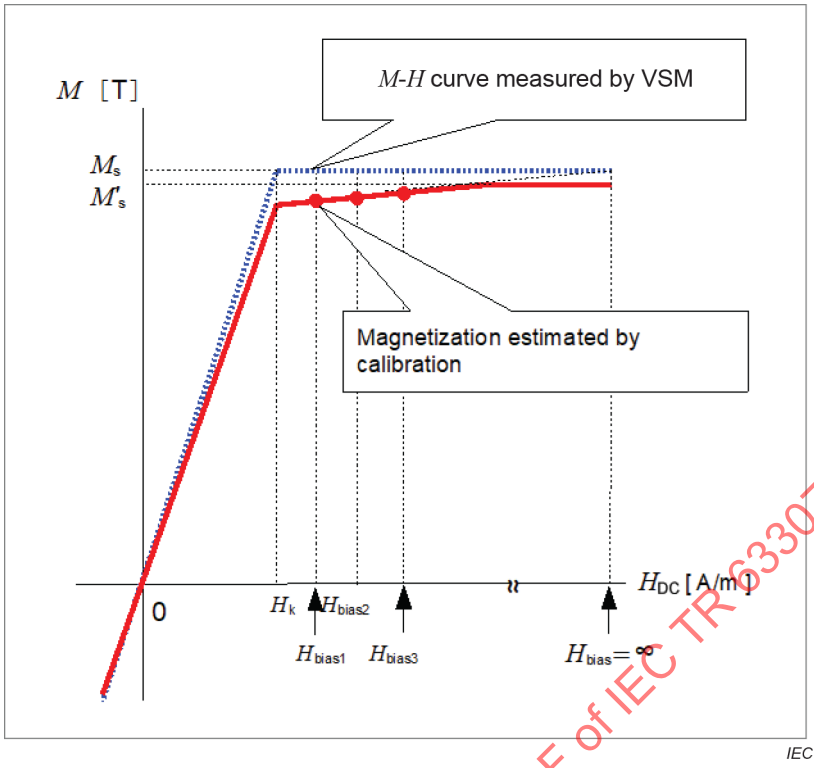

Figure 27 – DC magnetization curve

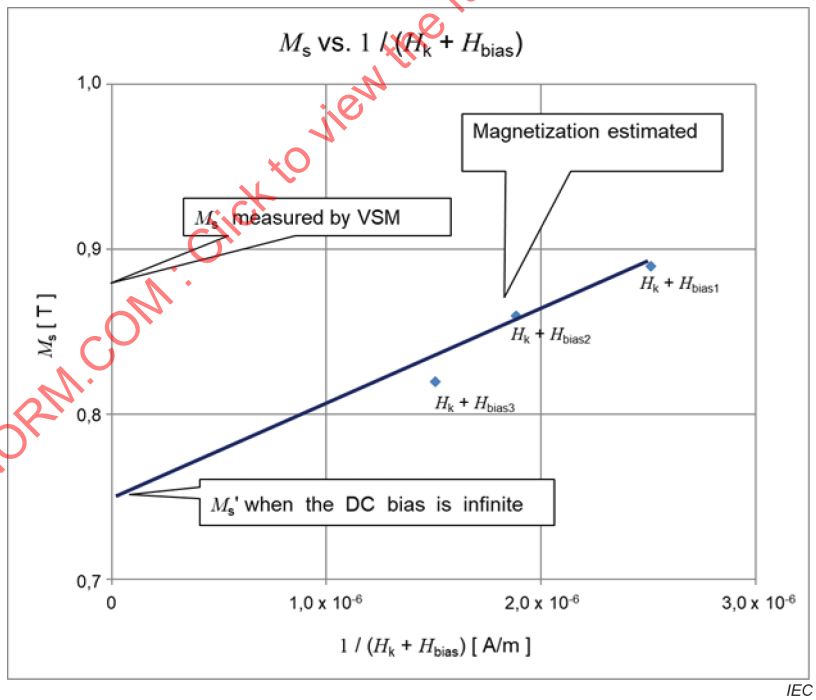

Figure 28 – Estimation of absolute value correction coefficient M'_s

5.5.2 Measurement frequency and accuracy

This method is useful to evaluate the relative permeability of a thin-film and sheet-like magnetic material. The measurement frequency range is as follows. Highly accurate data can be obtained along the hard axis of magnetization if a NSS sample has magnetic anisotropy in the plane.

Frequency range: 1 MHz ≤ f ≤ 10 GHz

IECNORM.COM : Click to view the full PDF of IEC TR 63307:2020

Accuracy: value error ±5 %

5.5.3 Measurement parameters

$$\mu'_r, \mu''_r, \text{ and } \mu_r$$

where:

$\mu_r = \mu'_r - \mu''_r$

5.5.4 NSS sample dimension and recommendation

Figure 29 explains the NSS sample dimension. The NSS sample should be sized to be inserted into the window of the shielded loop coil. The NSS sample can be attached to glass, quartz, or polyimide substrate. Avoid conductive material as the substrate.

Since the cross-sectional area of the NSS sample S_m (width x thickness, excluding the substrate) is used for Formula (31) and (32), it is necessary to measure the NSS sample width and thickness within an error of 5/100 mm or less in order to maintain measurement accuracy.

The NSS sample is for H_k < 7 958 [A/m].

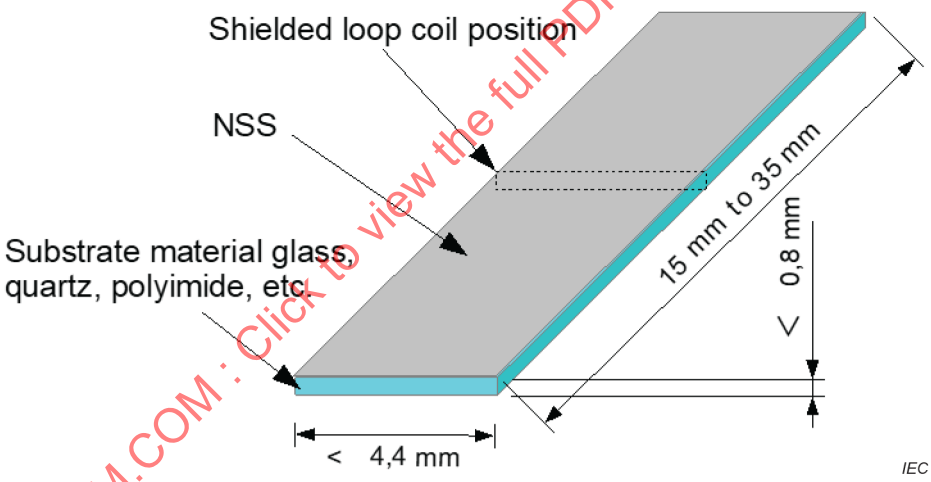

Measurement direction:	In-plane direction only. Both isotropic and anisotropic materials can be measured. Perpendicular direction to the sample surface (thickness direction) is not recommended.
NSS sample width:	4,4 mm or less.
NSS sample thickness:	0,8 mm or the less including substrate thickness (to be inserted in the measurement window).
NSS sample length:	4,0 mm or more (15 mm to 35 mm is recommended).

Figure 29 – Recommended shape of NSS sample

IECNORM.COM : Click to view the full PDF of IEC TR 63307:2020

5.5.5 Measurement environment

Measurement environment preference:

At room temperature 23 °C ± 5 °C

Humidity at 70 % or less

Cables and connectors:

The connecting section of APC 3,5 mm connectors used for connecting the cables of the measurement system should be cleaned up by removing metal wastes. Tighten the connector with the torque specified by the torque wrench. Bending of the measurement cable should be within the specification range of the cable. Avoid any movement of the cable after calibrating the measurement system, however tiny it will be.

5.5.6 Measurement system

Figure 30 shows the measurement block diagram of this equipment. A 13,5 GHz network analyzer and a DC power supply are controlled by PC via a GP–IB interface.

The DC power supply feeds electric current to a solenoid coil to generate H_{DC}.

The reflection port of the network analyzer is connected to a port of a TEM cell through an RF cable, giving a uniform magnetic field to the NSS sample by an RF signal from the network analyzer. The other port of the TEM cell is terminated by a 50 Ω resistor. The transmission port of the network analyzer is connected to the shielded loop coil that detects the magnetic flux of the NSS sample. Cooling water is used to cool down the solenoid coil and not to heat up the NSS sample from the surrounding environment.

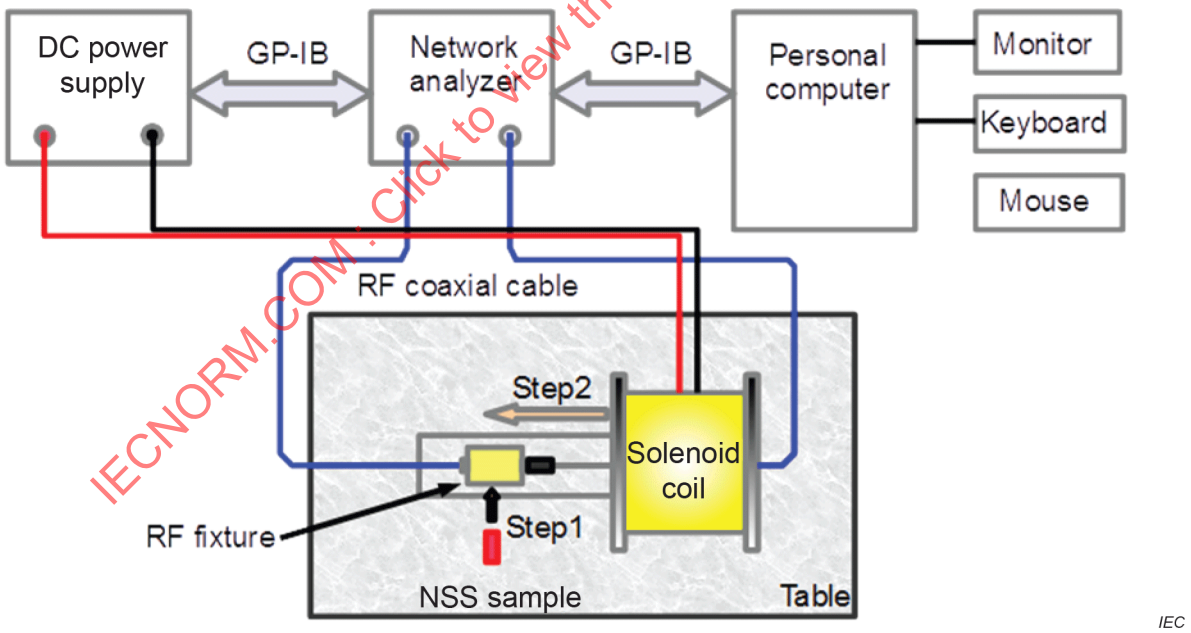

Figure 30 – Block diagram of measurement system

5.5.7 Measurement procedure

5.5.7.1 Overall procedure

1) Measure M_s and H_k of the NSS sample before the relative permeability measurement using a VSM (vibrating sample magnetometer) or similar equipment.
2) Perform a full two-port calibration of the network analyzer.

IECNORM.COM : Click to view the full PDF of IEC TR 63307:2020

3) Insert the NSS sample in the measurement unit as shown in Figure 30 by the arrow Step1.
4) Slide the solenoid coil in the Step2 direction until the end to cover the measurement unit.
5) Start a relative permeability measurement using the application software on the PC.
6) Perform a set of reference and main measurements. Note that the only difference between the two measurements is the presence/absence of the external DC magnetic field H_{DC}. Completion of this step gives complex relative permeability without magnetic calibration (absolute value calibration) based on Formula (32).
7) Apply magnetic calibration (absolute value calibration) as described in the steps 1) to 5) in 5.5.1.4.5. Completion of this step gives complex relative permeability with magnetic calibration (absolute value calibration) based on Formula (34).

5.5.7.2 Example of detailed absolute value calibration procedure

1) Make sure that M_s and H_k of the NSS sample are measured before the relative permeability measurement using a VSM or similar equipment.
2) Set several DC external magnetic field intensities H_{biasi} of the user's choice in the range of $H_k < H_{biasi} << H_{sat}$.
3) Measure the complex relative permeability by applying the same procedure as the main measurement.

   In Figure 27, three bias points (i = 1, 2, 3) are selected, and the corresponding DC external magnetic fields $H_{dc} = H_{bias1}$, H_{bias2} and H_{bias3} are applied to the NSS sample to measure relative permeability μ'_{r1}, μ'_{r2} and μ'_{r3}, respectively.
4) Calculate the estimate of saturated magnetization M'_{si} at each bias point (i = 1, 2, 3), using Formula (33). Formula (35) is the same as Formula (33) in principle with a popular SI unit conversion.

$$M'_{si} = (H_k + H_{biasi}) \cdot \mu'_{ri} / 10\,000\ [\mathrm{T}] \quad (i = 1, 2, 3) \tag{35}$$

5) Plot each M'_{si} on the graph whose horizontal axis is 1 / (H_k + H_{biasi}) and vertical axis is M'_{si} [T] (Figure 25). Let M'_s be the estimate of saturated magnetization which can be found by extrapolating the plot to the point where 1 / (H_k + H_{biasi}) = 0. If the plots do not align on a straight line, use the least squares method to estimate the zero point.
6) Find the calibration coefficient as M_s / M'_s. The calibrated complex relative permeability is obtained by multiplying this calibration coefficient M_s / M'_s to the real part μ'_{rob} and imaginary part μ''_{rob} of the complex relative permeability, as shown in Formula (34).

5.5.8 Measurement results

Figure 31 to Figure 35 show the measured results of the complex relative permeability. Table 2 lists the sample details. Sample A-01 was measured in a range from 1 MHz to 13,5 GHz. The sample sizes are 4 mm × 4 mm and 4 mm × 35 mm, respectively.

μ'_r, μ''_r, and μ_r

NOTE The legends in each figure give the meaning of each line color.

The different relative permeability profiles of the two samples of a same material and the different sizes of 4 mm × 4 mm and 4 mm × 35 mm provide a comparison of the influence of the demagnetizing field due to the sample shape.

The maximum of the real part of the complex relative permeability of the 4 mm × 4 mm sample is 44. It is 112 for the 4 mm × 35 mm sample.

IECNORM.COM : Click to view the full PDF of IEC TR 63307:2020

Figure 32 shows the real part of the complex relative permeability of the noise suppression sheet Sample B-01 measured at 1 MHz to 13,5 GHz. The sample size was 4 mm × 4 mm and 4 mm × 35 mm, respectively.

The maximum of the real part of the complex relative permeability of the 4 mm × 4 mm sample is about 25 and the relative permeability of the 4 mm × 35 mm sample is 54.

As with Sample A, two samples of a same material and different sizes are compared to see the influence of the demagnetizing field.

Figure 33 shows the DC bias magnetic field dependence of the complex relative permeability of the noise suppression sheet Sample A-02 measured between 1 MHz to 13,5 GHz. The sample size is 4 mm × 15 mm.

Table 2 – Measurement sample table

Sample name	Sample size	Thickness	Figure no.
Sample A-01	4 mm × 4 mm	100 µm	Figure 31
Sample A-01	4 mm × 35 mm	100 µm	Figure 31/Figure 34
Sample A-02	4 mm × 15 mm	200 µm	Figure 33
Sample B-01	4 mm × 4 mm	100 µm	Figure 32
Sample B-01	4 mm × 35 mm	100 µm	Figure 32/Figure 35

IECNORM.COM : Click to view the full PDF of IEC TR 63307:2020

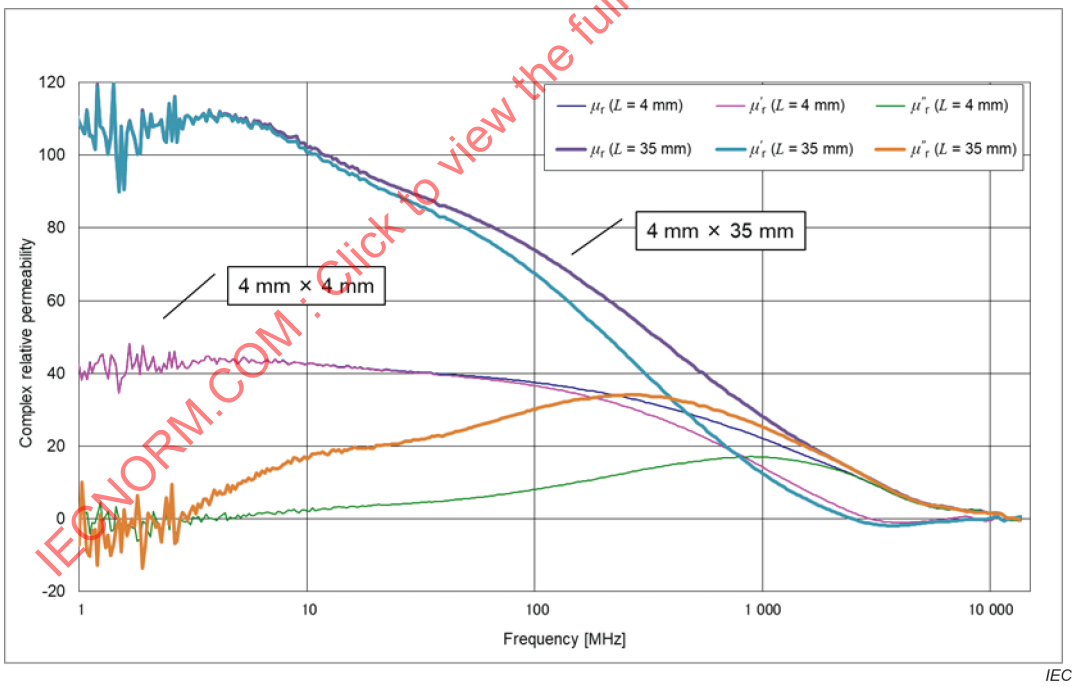

Figure 31 – Measured complex relative permeability as a function of the size of a NSS sheet (Sample A-01)

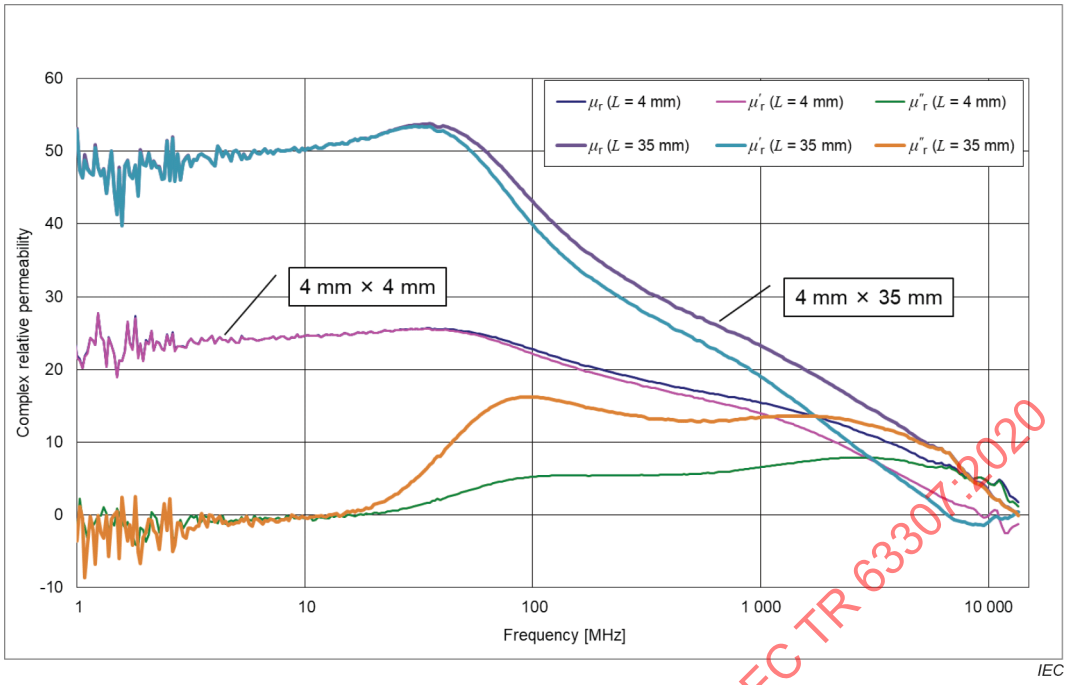

Figure 32 – Measured complex relative permeability as a function of the size of a NSS sheet (Sample B-01)

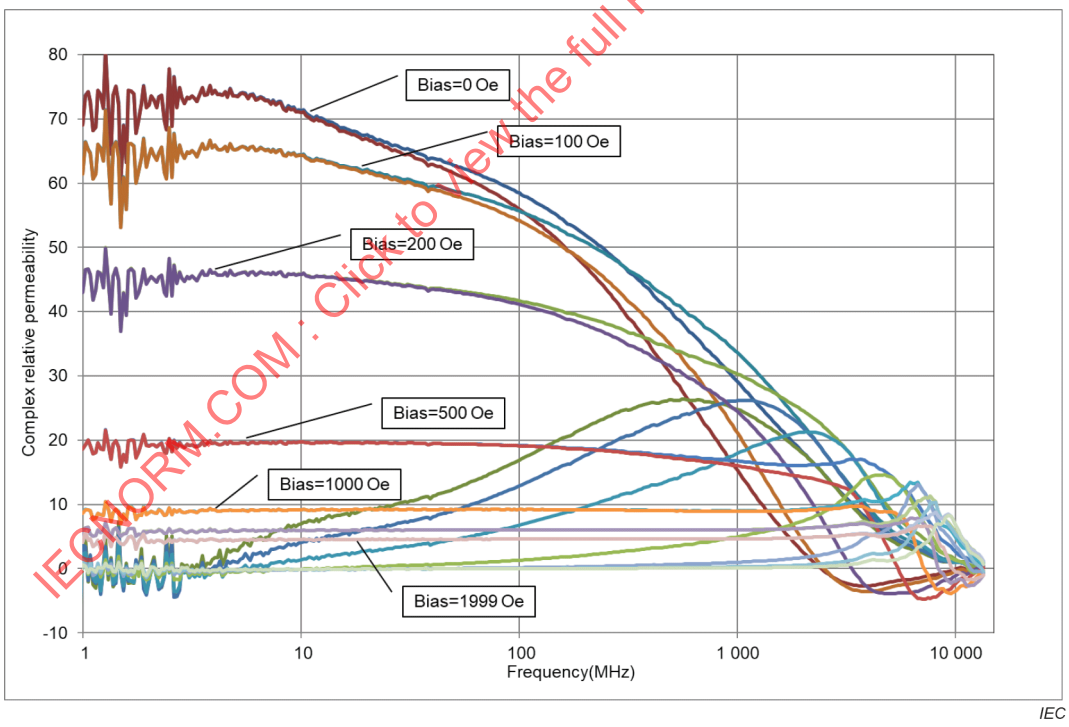

Figure 33 – Measured complex relative permeability of a NSS sheet as a function of DC bias field intensity (Sample A-02)

Figure 34 and Figure 35 show the calibrated complex relative permeability of two types of the Samples A-01 and B-01 obtained by applying the bias magnetic field as described in 5.5.1.4.5.

The noise on the low frequency side increases due to the sensitivity of the coil.

This system can also filter low frequency noise for removal.

IECNORM.COM : Click to view the full PDF of IEC TR 63307:2020

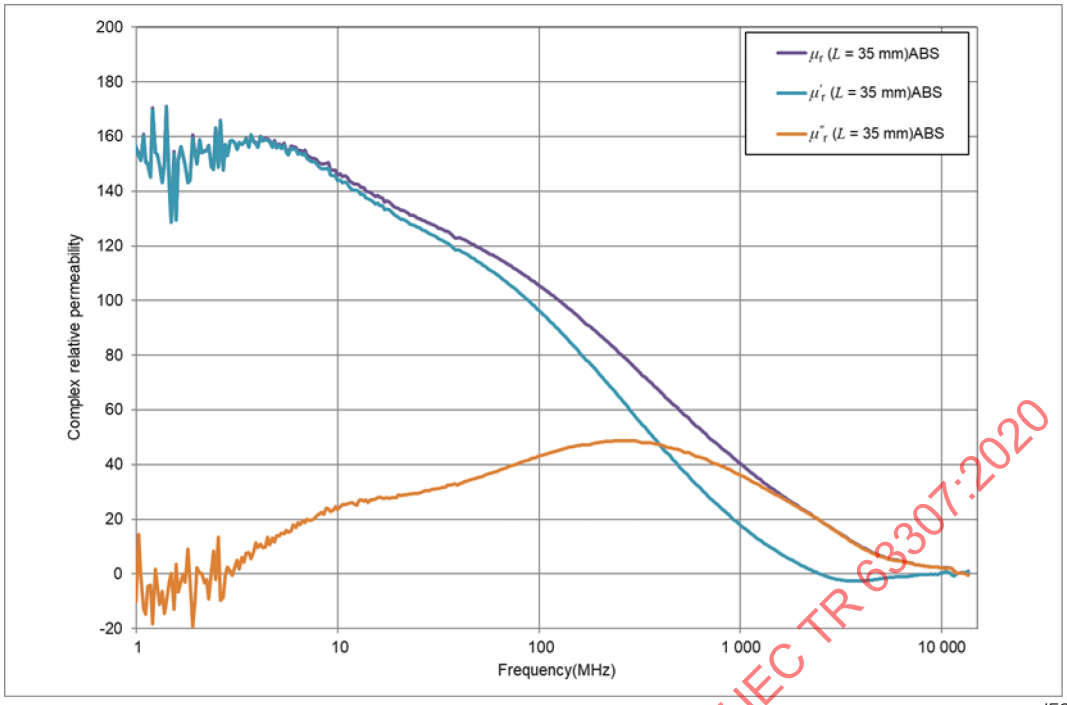

Figure 34 – Measured complex relative permeability after absolute value calibration (Sample A-01)

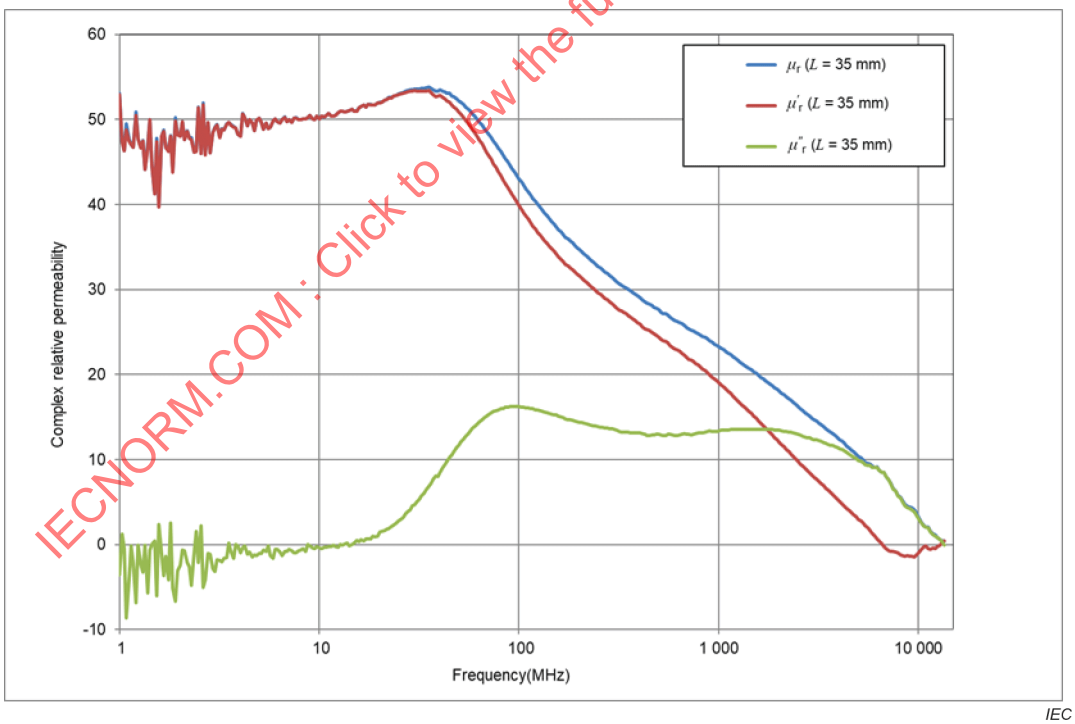

Figure 35 – Measured complex relative permeability after absolute value calibration (Sample B-01)

5.5.9 Summary

The shielded loop coil method has a degree of freedom in the shape of a sample since it measures a specimen of any size that can be enclosed in the window aperture at the centre of the coil.

IECNORM.COM : Click to view the full PDF of IEC TR 63307:2020

The relative permeability of a sample can be sensitive to the direction of applied bias and RF magnetic fields because of the anisotropic nature of magnetization. Accordingly there is also a direction in which highly accurate measurement can be made, depending on the direction of applied magnetic fields.

It is a useful nature of this method that the relative permeability corresponding to the actual size of the magnetic materials in devices is obtained because the shape-dependent demagnetizing field is counted in the measurements. If a user needs relative permeability inherent in the material, a sample long enough along the measurement direction is used.

In order to calibrate measurement errors caused by leakage magnetic flux from a sample, absolute value calibration is performed in this measurement.

Sample A-02 should suppress electromagnetic noise most at the frequency around 300 MHz where $\mu"_r$ in Figure 31 has the maximum value.

Sample B-01 in Figure 35 should have good noise suppression effect between 50 MHz and 5 GHz where $\mu"_r$ is high.

5.6 Harmonic resonance cavity perturbation method

5.6.1 Theory

An exchange between magnetic and electric energies occurs after an electromagnetic stimulus is given from a small aperture to a metal closed cavity. This is called the natural resonance, and the resonance will be decreased by the cavity wall's energy loss. If the stimulus is applied with the same interval as the energy exchange, the energy in the cavity increases until the energy loss in the cavity becomes the same as the external energy supplied. This is called electromagnetic resonance. The electric field strength in the cavity is null where the magnetic field strength is the maximum and vice versa. A material installed in the magnetic field maximum part shifts the resonance characteristics in proportion to the magnetic characteristics. A small sample in the cavity gives a fractional change in the resonance frequency as shown in Formula (36)

$$\frac{\Delta\omega}{\omega_0} = -\frac{\Delta W}{W_0} \tag{36}$$

where

$\Delta\omega$ is the shift in the angular resonance frequency;

ω_0 is the angular resonance frequency of the blank cavity;

ΔW is the change in the stored energy;

W_0 is the stored energy of the blank cavity.

The electromagnetic expression of the above terms is shown as follows:

$$\Delta W = \int_{\Delta v} \left[\varepsilon_0 (\varepsilon'_r - 1) E \cdot E^* + \mu_0 (\mu'_r - 1) H \cdot H^* \right] dv \tag{37}$$

where

E is the electric field strength;

H is the magnetic field strength;

Δv is the sample volume;

IECNORM.COM : Click to view the full PDF of IEC TR 63307:2020

ε_r is the complex relative permittivity of the material: $\varepsilon_r = \varepsilon'_r - j\varepsilon''_r$;

μ_r is the complex relative permeability of the material: $\mu_r = \mu'_r - j\mu''_r$.

The asterisk shows the complex conjugate of the field vector and the terms in square brackets are integrated over the volume of the sample.

$$W_0 = \frac{1}{2}\int_V \left[\varepsilon_0 \mathrm{E}\cdot E^* + \mu_0 H \cdot H^*\right] dv \tag{38}$$

where the integral is over the volume of the cavity.

V is the volume of the cavity.

The resonance cavity perturbation method is a classical method and it enables the permeability evaluation over a broad frequency range using the same sample in the range of different cavities of different resonance frequencies. After a small sample is put into a region of the strongest magnetic field strength and zero electric field strength parts of a cavity, the resonance frequency shifts proportionally to the magnetic susceptibility of the material (μ'_r) and the cavity loss factor increases with the loss of the material (μ''_r). [1][1] The perturbation evaluated in the cavity with a small coupling factor indicates that the connected loads at the outside will have a small influence on the results.

5.6.2 Permeability evaluation

5.6.2.1 General

If the sample is small and located in the regions of a maximum of H and an electric field strength E of zero in the cavity, the energy change in the cavity is proportional to the permeability of the sample. The method to characterize the material as shown above is called the resonance cavity perturbation method. The permeability of the sample is written as shown in Formula (39)

$$\mu'_r = 1 + \frac{V}{\alpha \Delta v}\left(\frac{f_0 - f_s}{f_0}\right)$$
$$\mu''_r = \frac{V}{2\alpha \Delta v}\left(\frac{1}{Q_s} - \frac{1}{Q_0}\right) \tag{39}$$

where

V is the volume of the cavity;

Δv is the volume of the sample;

α is the factor defined by the sample position and the cavity mode;

f_0 is the resonance frequency of the blank cavity;

f_s is the resonance frequency of the sample installed cavity;

Q_0 is the Q factor of the blank cavity;

Q_s is the Q factor of the sample installed cavity.

IECNORM.COM : Click to view the full PDF of IEC TR 63307:2020

[1] Numbers in square brackets refer to the Bibliography.

The formula shows that the real part of the permeability is described by the resonance frequency shift ratio and the imaginary part is described by the increase of the cavity loss. A clear one-to-one relationship between the complex permeability and the frequency shift ratio or the loss increase is confirmed by the formula, and the measurement accuracy of the resonance characteristic is essential in the permeability evaluation.

The resonance cavity perturbation method has been established for a resonance cavity of a single resonance frequency and the permeability measurement for one frequency was considered. If a rectangular waveguide TE_{012} cavity is used as the resonance cavity, the regions of a maximum of H and an electric field strength E of zero are found at the centre and ends of the cavity as shown in Figure 36 (Position 1 and Position 2). Therefore no magnetic field is applied to both ends of the sample. The installation of the sample in this area of intrinsic permeability is evaluated without the depolarization field.

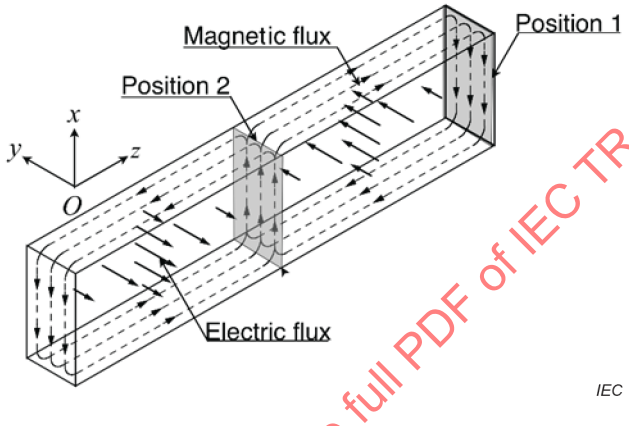

Figure 36 – Electromagnetic flux to evaluate permeability in the harmonic resonance cavity resonator

Two examples for the resonance characteristics change are shown in Figure 37. Figure 37a) shows the resonance curve change observed in the single frequency resonator. Figure 37b) shows the resonance frequency change in a cavity with two resonance frequencies.

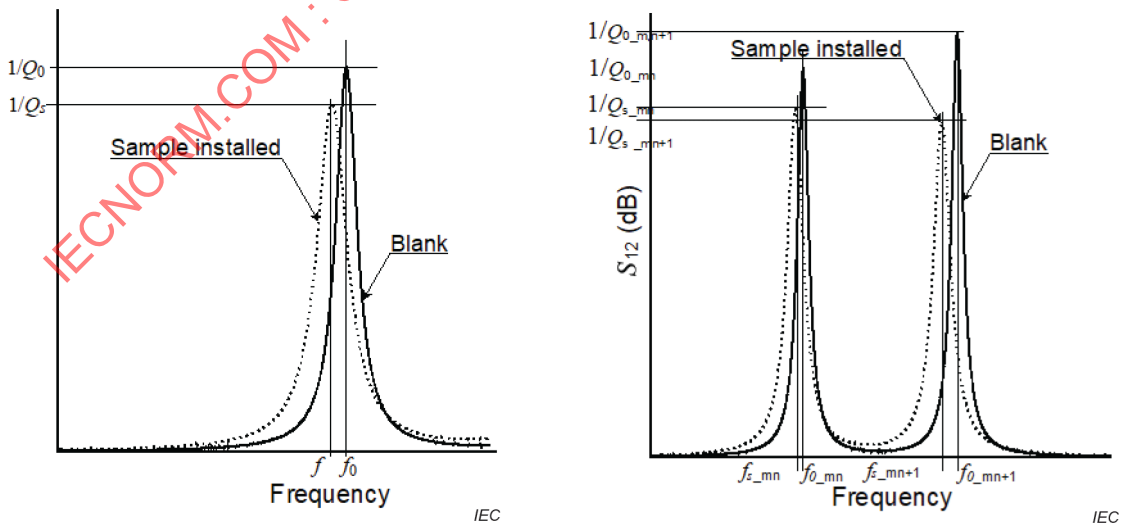

a) Single resonance frequency **b) Two resonance frequencies cavity**

Figure 37 – Example of the resonance characteristics change

IECNORM.COM : Click to view the full PDF of IEC TR 63307:2020

A rectangular waveguide shorted at both ends will resonate at those frequencies for which the length is equal to an integral multiple of a half wavelength in the waveguide. If only a single mode such as TE_{10} is found in the waveguide, this can be called a harmonic resonance cavity because the resonance will be observed at the harmonic number, n, of the waveguide mode [22]. It is proposed here to use the resonator to evaluate the frequency characteristics of materials by the resonance cavity perturbation method. The dimensions of the waveguide resonator become very big at values lower than 2 GHz. A TEM-mode resonator is appropriate in this frequency range but the magnetic field distribution of the TEM-mode resonator with a single line is not the same as the waveguide resonator. The magnetic field distribution of a TEM-mode resonator with two parallel plates as the centre conductor is the same as that shown in Figure 34. This structure of the resonator was used at the frequency range from 250 MHz to 2 GHz. Examples of the structure of the resonators and the resonance frequencies are shown in Figure 38 and Figure 39 respectively.

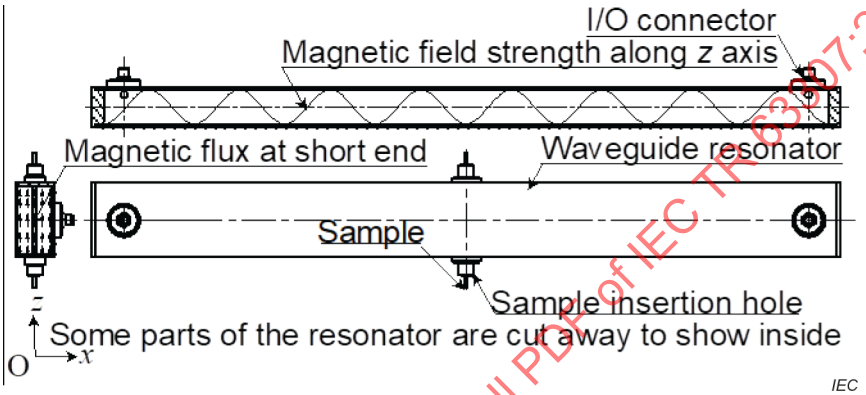

Figure 38 – Cavity resonator for 3,6 GHz to 7,2 GHz

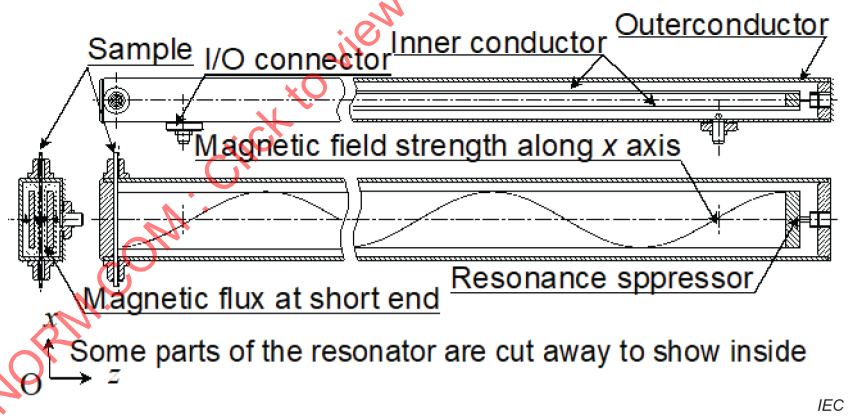

Figure 39 – Cavity resonator for 0,25 GHz to 2 GHz

The numbers of the resonance frequencies in the band are defined by the length of the resonator. A longer resonator length increases the numbers of the resonance frequencies in the band and gives accurate frequency characteristics of the material. However, a small difference between the resonance frequencies makes it difficult to evaluate the frequency shift caused by the insertion of the sample. Four to eight resonance frequencies in the band are appropriate. Examples are shown in Figure 40.

IECNORM.COM : Click to view the full PDF of IEC TR 63307:2020

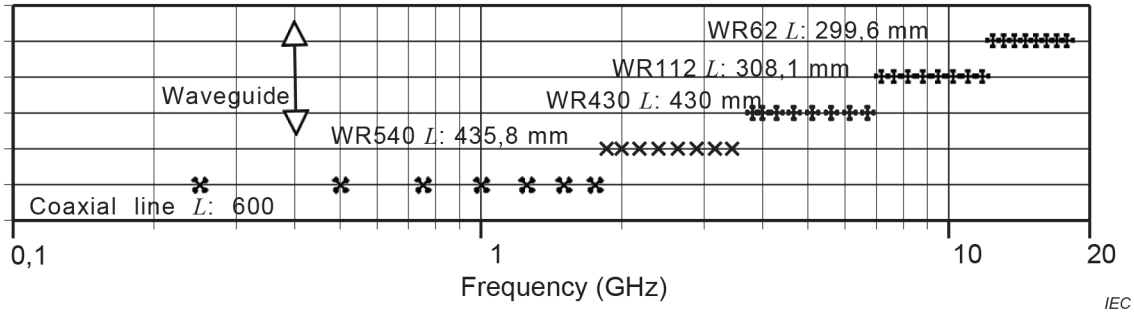

Figure 40 – Examples of resonance frequencies

An example of the harmonic resonance curves in the C-band is shown in Figure 41.

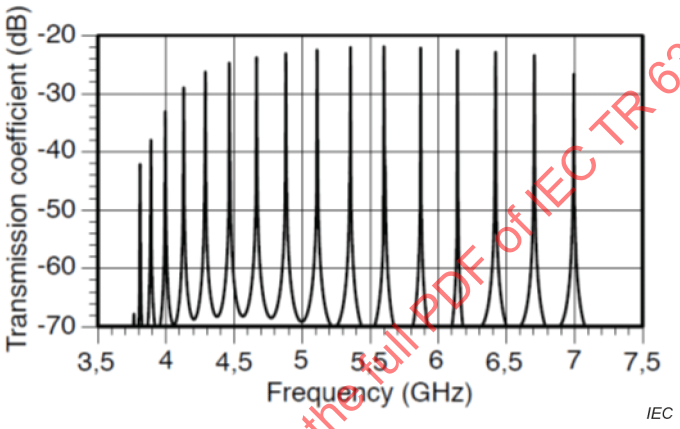

Figure 41 – Example of the resonance curves of a harmonic resonance cavity

5.6.2.2 Measurement frequency and accuracy

Frequency	:	250 MHz ≤ f ≤ 18 GHz
Relative permeability	:	$-5 \leq \mu'_r \leq 50$
		$0,1 \leq \mu''_r \leq 10$
		x, y or z axis
Accuracy	:	order of significant digits: 2

5.6.2.3 Sample dimensions

5.6.2.3.1 Permeability evaluation parallel to the plane

Cut out a tape.

Width: < 2 mm

Thickness: < 2 mm

Length: > 100 mm

5.6.2.3.2 Permeability evaluation orthogonal to the plane

Punch out small disks and stack.

Diameter: < 2 mm

Length: > 50 mm

IECNORM.COM : Click to view the full PDF of IEC TR 63307:2020

The samples prepared as described above are shown in Figure 42 as examples.

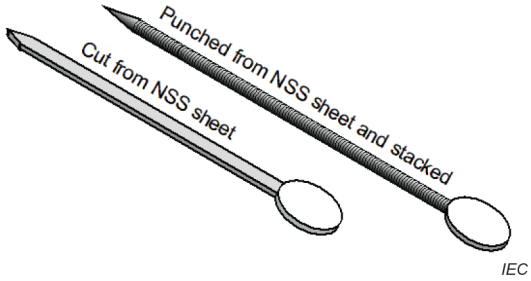

Figure 42 – Examples of samples

5.6.2.4 Environment

Room temperature: 15 °C to 35 °C.

5.6.2.5 Apparatus

5.6.2.5.1 General

The measuring system of the permeability of the NSS is constructed by the network analyzer, and the harmonic resonance cavity resonates in the defined frequency band (see Figure 43).

5.6.2.5.2 Network analyzer

The frequency range of the network analyzer should cover the resonance frequency of the harmonic resonance cavity resonator, and the dynamic range of the analyzer should be more than 40 dB.

5.6.2.5.3 Test fixture

The resonance frequencies of the harmonic resonance cavity should have enough numbers of the resonance frequency to evaluate the frequency characteristics of NSS; more than six resonance frequencies in the band would be a good number. A personal computer used to calculate the complex permeability from the data given by the network analyzer should be provided.

IECNORM.COM : Click to view the full PDF of IEC TR 63307:2020

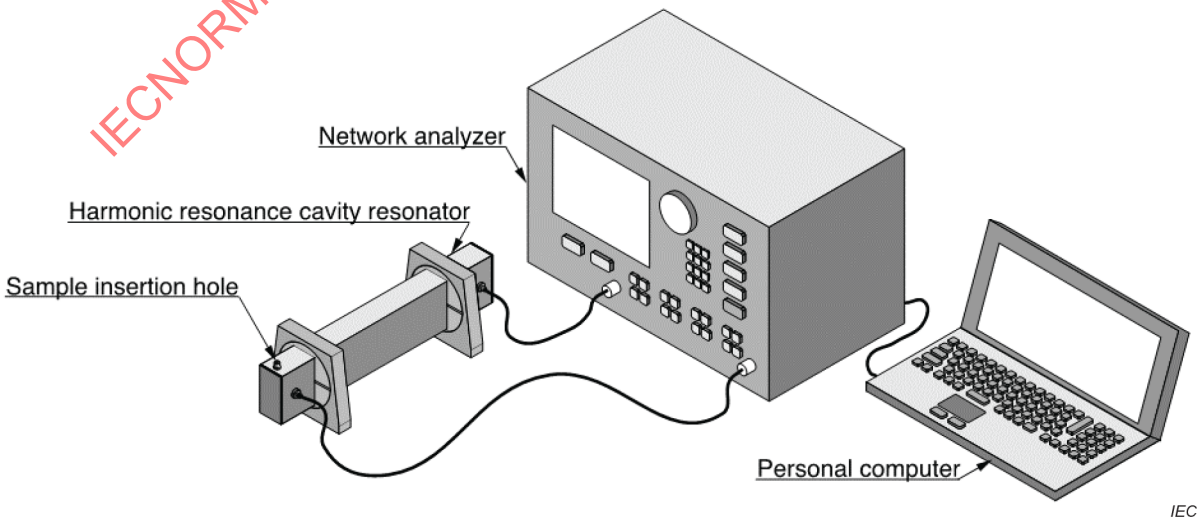

Figure 43 – Measuring system

5.6.2.6 Measurement procedure of permeability

5.6.2.6.1 Resonance characteristics (f_{0_mn} and Q_{0_mn}) evaluation of the blank cavity

5.6.2.6.1.1 General

The resonance frequency, f_{0_mn} and the Q factor, Q_{0_mn}, of the blank cavity are measured. The suffix mn means n-th resonance frequency or the Q factor in the m-band cavity.

5.6.2.6.1.2 f_{REF_mn}, the n-th resonance frequency of the m-band cavity

Resonance frequency, f_{REF_mn}, of the reference sample installed cavity is measured to define the proportional factor. The suffix mn means the n-th resonance peak in the m-band cavity.

5.6.2.6.1.3 Calibration factor (α_{mn}) definition of the cavity

The proportional factor α_{mn} is given by inserting a nonmagnetic good conductor as a reference sample because the permeability of the good conductor is 0 in this frequency range. A copper rod will be favourable as a good conductor. The proportional factor α_{mn} is calculated by the obtained data and the following formula:

$$\alpha_{mn} = \frac{V}{\Delta v_{REF}} \left(\frac{f_{REF\_mn} - f_{0\_mn}}{f_{0\_mn}} \right) \tag{40}$$

where

V is the volume of the cavity;

Δv_{REF} is the volume of the reference sample in the cavity;

f_{0_mn} is the n-th resonance frequency in the m-band vacant cavity;

f_{REF_mn} is the n-th resonance frequency in m-band cavity with the reference sample.

5.6.2.6.2 Sample installation

Insert the sample into the sample installation hole of the cavity as shown in Figure 44.

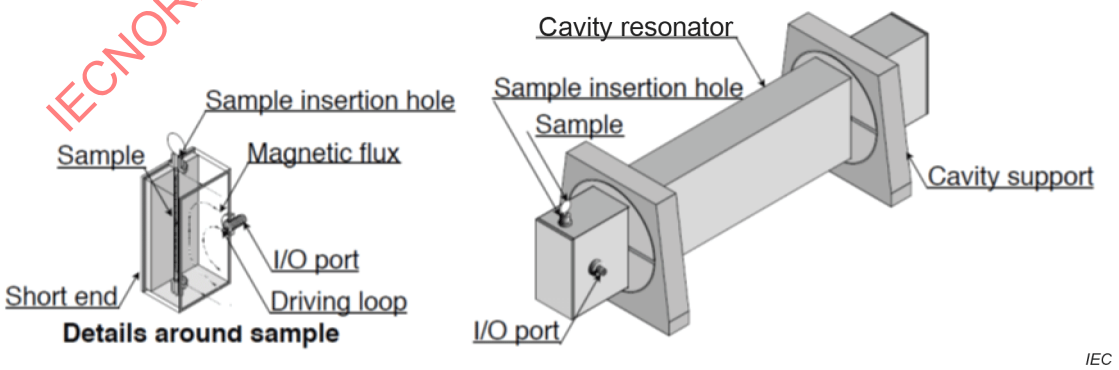

Figure 44 – Sample installation in the cavity for the permeability measurement

IECNORM.COM : Click to view the full PDF of IEC TR 63307:2020

5.6.2.6.3 Resonance characteristics (f_{s_mn} and Q_{s_mn}) evaluation of the sample

The resonance frequency, f_s, and the Q factor, Q_s, of the cavity installing the sample are measured by a network analyzer. The suffix mn means the resonance characteristics of the n-th resonance frequency in the m-band cavity.

5.6.2.6.4 Calculation of the permeability

The real part and the imaginary part of the relative permeability of the n-th resonance frequency of the m-band cavity are given as shown in Formula (41) and (42), respectively.

$$\mu'_{r\_mn} = 1 + \frac{V}{\alpha_{mn}\Delta v}\left(\frac{f_{0\_mn} - f_{s\_mn}}{f_{0\_mn}}\right) \tag{41}$$

$$\mu''_{r\_mn} = \frac{V}{2\alpha_{mn}\Delta v}\left(\frac{1}{Q_{s\_mn}} - \frac{1}{Q_{0\_mn}}\right) \tag{42}$$

where

V is the volume of the cavity;

Δv is the volume of the sample in the cavity;

α_m is the proportional constant;

f_0 is the resonance frequency of the empty cavity;

f_s is the resonance frequency of the sample installed cavity;

Q_0 is the Q factor of the empty cavity;

Q_s is the Q factor of the sample installed cavity.

5.6.2.7 Expression of the results

The obtained results are plotted in terms of the measured frequency and the complex relative permeability as shown in Figure 45. The permeability of a good conductor is 0. If a good conductor is included in the sample, the consistency of the measurement is confirmed and the deviation of the relative permeability of the conductor from 0 corresponds to the accuracy of the measurement. Permeability_xy is the permeability in the sheet plane. Permeability_z is the permeability perpendicular to the sheet. The subscript after the under score is the sample name.

IECNORM.COM : Click to view the full PDF of IEC TR 63307:2020

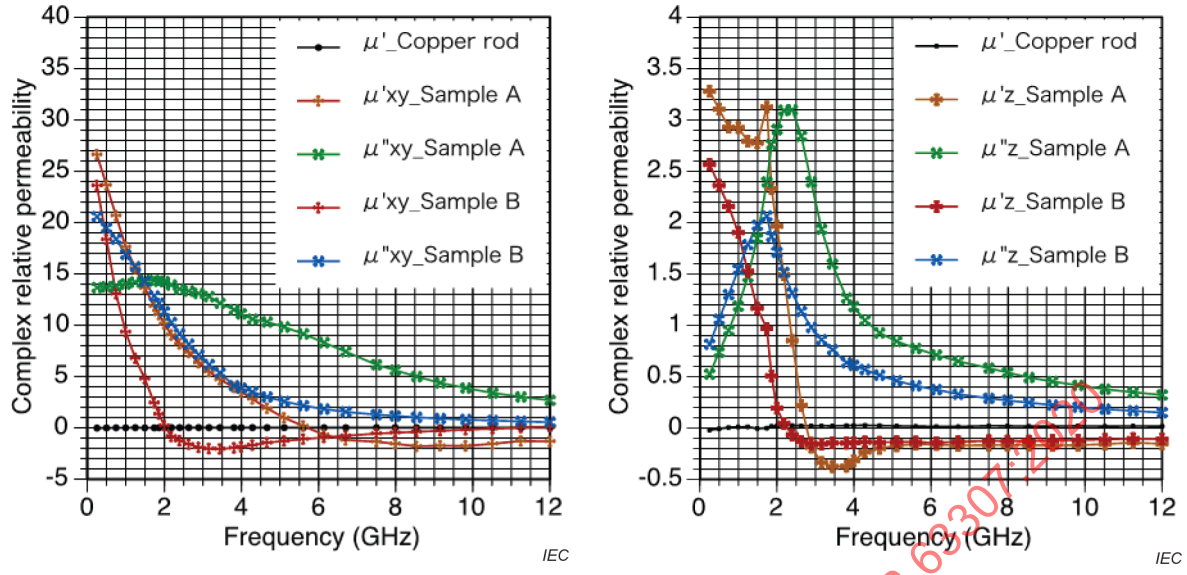

a) Permeability_xy

b) Permeability_z

Figure 45 – Measured results of the permeability for Sample A and B and a copper rod

5.6.3 Permittivity evaluation

5.6.3.1 General

The permittivity of the NSS material is strongly frequency dependent and anisotropic, just as the permeability of the NSS is strongly frequency dependent and anisotropic.

If a small sample is installed at the region of the maximum electric field strength and the magnetic field strength is zero in the cavity as shown in Figure 46, the energy change in the cavity is proportional to the permittivity of the sample. The method to characterize the material as shown above is called the resonance cavity perturbation method [21].

IECNORM.COM : Click to view the full PDF of IEC TR 63307:2020

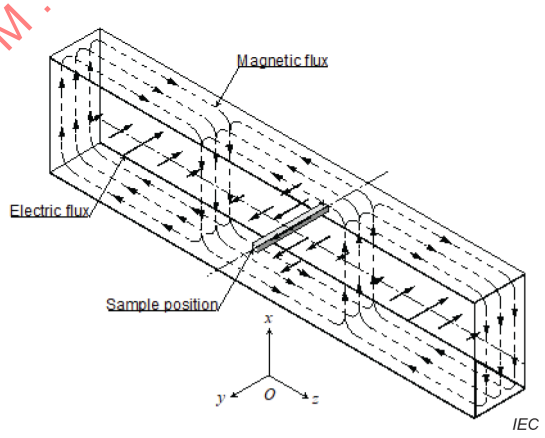

Figure 46 – Electromagnetic flux to evaluate permittivity in the harmonic resonance cavity resonator

The evaluation of the permittivity will be carried out by the same procedure as the permeability was evaluated. The permittivity of the sample is described as shown in Formula (43). The suffix mn means the n-th resonance frequency or the Q factor in the m-band cavity.

$$\varepsilon'_{r\_mn} - j\varepsilon''_{r\_mn} = 1 + \frac{V}{2\Delta v}\left(\frac{f_{0\_mn} - f_{S\_mn}}{f_{0\_mn}}\right) - j\frac{V}{4\Delta v}\left(\frac{1}{Q_{s\_mn}} - \frac{1}{Q_{0\_mn}}\right) \quad (43)$$

where

V is the volume of the cavity;

Δv is the volume of the sample in the cavity;

f_0 is the resonance frequency of the empty cavity;

f_s is the resonance frequency of the sample installed cavity;

Q_0 is the Q factor of the empty cavity;

Q_s is the Q factor of the sample installed cavity.

The formula shows that the real part of the permittivity is described by the resonance frequency shift ratio and the imaginary part is described by the increase of the cavity loss. A clear one-to-one relationship between the resonance frequency change and the loss increase is confirmed by the formula. The formula above shows that the accuracy of the resonator characteristics is essential to evaluate the permittivity.

Formerly, the resonance cavity perturbation method has been established for the resonance cavity of single resonance frequency and the permittivity measurement for one frequency was considered. The permittivity measurement by the harmonic resonance cavity enabled to evaluate the frequency dependent permittivity of the materials. If a rectangular waveguide TE_{013} cavity is used as the resonance cavity, the region of the maximum electric field strength E and the magnetic field strength H of zero is found at the centre of the cavity if the cavity resonates as shown in Figure 46. Certain electric field disturbances will occur at the sample insertion holes provided at the top and the bottom of the cavity. The disturbance of the electric field becomes the depolarization field of the sample and the adjustment of the depolarization will be required after the measurement.

IECNORM.COM : Click to view the full PDF of IEC TR 63307:2020

5.6.3.2 Measurement frequency and accuracy

Frequency	:	1,8 GHz ≤ f ≤ 8 GHz
Relative permeability	:	1 ≤ ε'_r ≤ 2 000
		0,001 ≤ ε''_r ≤ 300
		x, y or z axis
Accuracy	:	order of significant digits: 2

5.6.3.3 Sample dimensions

5.6.3.3.1 Permittivity parallel to the plane

Cut out a tape.

Width < 2 mm

Thickness < 2 mm

Length > 100 mm

5.6.3.3.2 Permittivity orthogonal to the plane

Punch out small disks and stack.

Diameter < 2 mm

Length > 50 mm

5.6.3.4 Environment

Room temperature is 15 ˚C to 35 ˚C.

5.6.3.5 Apparatus

Network analyzer

Test fixture

5.6.3.6 Measurement procedure of the permittivity

5.6.3.6.1 Resonance characteristics (f_{0_mn} and Q_{0_mn}) evaluation of the blank test fixture

Measure the resonance frequency f_{0_mn} and the Q factor Q_{0_mn} of the cavity where m is the measurement band, S or C, and n is the order of the resonance peak in the band.

5.6.3.6.2 Sample installation

Insert the sample into the sample installation hole of the cavity as shown in Figure 47.

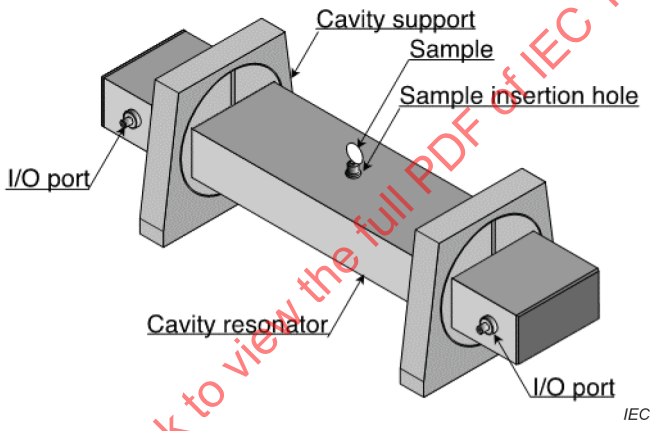

Figure 47 – Sample installation in the cavity for the permittivity measurement

5.6.3.6.3 Resonance characteristics (f_{s_mn} and Q_{s_mn}) evaluation of the sample

Measure the resonance frequency f_{mn} and the Q factor Q_{s_mn} of the sample installed cavity. The suffix m is the measurement band, S or C, and n is the order of the resonance peak in the band.

5.6.3.6.4 Calculation of the permeability

The relative permeability of the n-th resonance frequency of the m band cavity is given as follows

$$\varepsilon'_{r\_mn} = 1 + \frac{V}{2\Delta v}\left(\frac{f_{0\_mn} - f_{s\_mn}}{f_{0\_mn}}\right) \tag{44}$$

$$\varepsilon''_{r\_mn} = \frac{V}{4\Delta v}\left(\frac{1}{Q_{s\_mn}} - \frac{1}{Q_{0\_mn}}\right) \tag{45}$$

IECNORM.COM : Click to view the full PDF of IEC TR 63307:2020

where

V is the volume of the cavity;

Δv is the volume of the sample in the cavity;

f_0 is the resonance frequency of the m-band blank cavity;

f_s is the resonance frequency of the m-band sample installed cavity;

Q_{0_mn} is the n-th Q factor of the m-band vacant cavity;

Q_{s_mn} is the n-th Q factor of the m-band sample installed cavity.

5.6.3.7 Adjustment of the permittivity decrease caused by the depolarization field

The measurements of the permittivity are carried out by the resonators constructed by the rectangular waveguide resonators for the S-band and C-band. Examples of the measurement and the adjusted results are shown in Figure 48a) and Figure 48b), respectively.

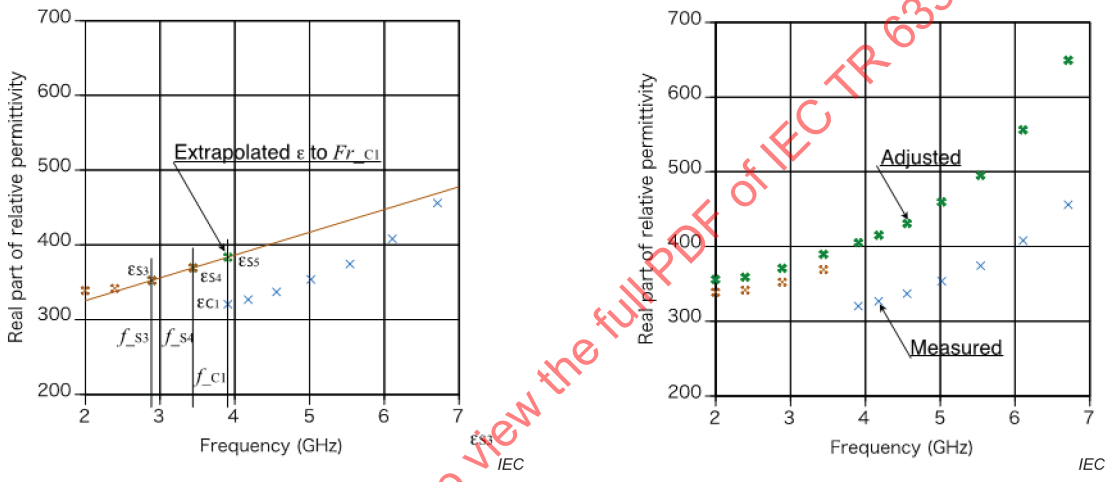

a) Adjustment procedure b) Adjusted results

Figure 48 – Adjustment procedure and adjusted results

Adjustment of the permittivity by using the results of two cavities with different heights has been carried out as follows.

1) Calculate the polarizability $\chi'=\varepsilon'-1$.
2) Estimate the polarizability χ'_{S5_meas} at f_{C1} by extrapolating χ'_{S3_meas} and χ'_{S4_meas}

$$\chi'_{S5} = \varepsilon'_{S5\_meas} - 1 = \frac{\varepsilon'_{S4\_meas} - \varepsilon'_{S3\_meas}}{f_{S4} - f_{S3}} (f_{C1} - f_{S3}) + \varepsilon_{S3\_meas} - 1 \quad (46)$$

3) χ'_{S5_meas} would be the polarizability if measured at f_{C1} in the S-band cavity.
4) The polarizability of the material measured at the S-band cavity with the cavity height, h_S, is χ'_{S_meas} and at the C-band cavity with the cavity height, h_C, is χ'_{C_meas}.
5) Suppose that the electrical length of the stick sample equals the cavity height, h_S or h_C, and the depolarization factor of the sample is inversely proportional to the length of the stick. The depolarization factors of the samples can be described as follows:

$$N_S = \frac{k}{h_S} \text{ and } N_C = \frac{k}{h_C} \quad (47)$$

IECNORM.COM : Click to view the full PDF of IEC TR 63307:2020

where

k is the proportional constant.

The proportional constant, k, is given by the formula shown below by using the measured polarizability χ'_{C1} and the supposed polarizability χ'_{S5}:

$$k = \frac{\frac{1}{\chi'_{C1\_meas}} - \frac{1}{\chi'_{S5\_meas}}}{\frac{1}{h_C} - \frac{1}{h_S}} \tag{48}$$

6) The real part of the adjusted dielectric constants at the measured frequencies can be calculated by using Formula (48) and the measured results as follows:

$$\varepsilon'_{Sn\_adjust} = \chi'_{Sn\_adjust} + 1 = \frac{\chi'_{Sn\_meas}}{1 - N_S \chi'_{Sn\_meas}} + 1 \tag{49}$$

$$\varepsilon'_{Cn\_adjust} = \chi'_{Cn\_adjust} + 1 = \frac{\chi'_{Cn\_meas}}{1 - N_C \chi'_{Cn\_meas}} + 1 \tag{50}$$

where

suffix S or C is the name of the band;

suffixes adjust and meas are the adjusted value and measured value;

n is the resonance frequency number in the bands.

7) The imaginary part of the adjusted dielectric constants at the measured frequencies can be calculated by using Formula (50) and the measured results are as follows:

$$\varepsilon''_{Sn\_adjust} = (1 + N_S \chi''_{Sn\_meas})^2 \tag{51}$$

$$\varepsilon''_{Cn\_adjust} = (1 + N_C \chi''_{Cn\_meas})^2 \tag{52}$$

5.6.3.8 Expression of the results

The adjusted results are shown in Figure 49. The suffixes in Figure 49 mean the direction of the electric field and the sample name, respectively.

IECNORM.COM : Click to view the full PDF of IEC TR 63307:2020

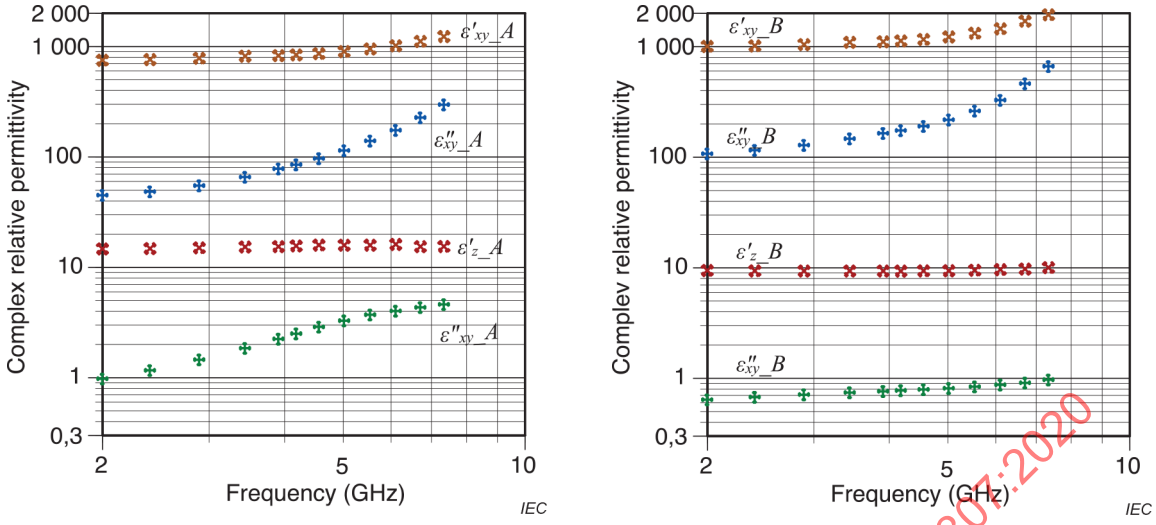

a) Permittivity of Sample A **b) Permittivity of Sample B**

Figure 49 – Measured results of the permittivity for the two samples, A and B

The seamless connections of the adjusted results are confirmed from the results above. Although no adjustment for the imaginary part has been carried out in the procedure, the seamless connection shown in the above results confirmed that the adjustment would be consistent.

IECNORM.COM : Click to view the full PDF of IEC TR 63307:2020

Annex A
(informative)

Derivation of the complex relative permeability of the inductance method

The self-inductance L of the one-turn coil in Figure 3 is expressed by:

$$L = \frac{Z}{\mathrm{j}\omega} = \frac{1}{I}\int_S B\,ds =$$

$$\frac{\mu_0}{2\pi}\left(\mu_\mathrm{r} - 1\right)\mathrm{F} + \frac{\mu_0}{2\pi}\mathrm{F}_0 =$$

$$\frac{\mu_0}{2\pi}\left(\mu_\mathrm{r}' - 1\right)\mathrm{F} - \mathrm{j}\frac{\mu_0}{2\pi}\mu_\mathrm{r}''\mathrm{F} + \frac{\mu_0}{2\pi}\mathrm{F}_0 =$$

$$\frac{x_{\mathrm{NSS}}}{\omega} - \mathrm{j}\frac{r_{\mathrm{NSS}}}{\omega} + L_{\mathrm{Short}} \tag{A.1}$$

where

$$F = h\,ln\left(\frac{b}{a}\right) \tag{A.2}$$

$$F_0 = h_0\,ln\left(\frac{b_0}{a_0}\right) \tag{A.3}$$

r_{NSS} and x_{NSS} are the real part and imaginary part of the self-inductance with the NSS sample. L_{Short} is the self-inductance without the NSS sample. They are given as follows, respectively:

$$r_{\mathrm{NSS}} = \omega\frac{\mu_0}{2\pi}\mu_\mathrm{r}''\mathrm{F} \tag{A.4}$$

$$x_{\mathrm{NSS}} = \omega L_{\mathrm{NSS}} = \omega\frac{\mu_0}{2\pi}\left(\mu_\mathrm{r}' - 1\right)\mathrm{F} \tag{A.5}$$

$$L_{\mathrm{Short}} = \frac{\mu_0}{2\pi}\mathrm{F}_0\,. \tag{A.6}$$

The impedance Z_{NSS} is due to the effect of the fixture and is expressed by the impedance of the fixture with and without the NSS sample, Z_m and Z_{sm}, as follows:

$$Z_{\mathrm{NSS}} = Z_\mathrm{m} - Z_{\mathrm{sm}} = r_\mathrm{m} - r_{\mathrm{sm}} + \mathrm{j}\left(x_\mathrm{m} - x_{\mathrm{sm}}\right) =$$

$$r_{\mathrm{NSS}} + \mathrm{j}\,x_{\mathrm{NSS}} = r_{\mathrm{NSS}} + \mathrm{j}\omega L_{\mathrm{NSS}} \tag{A.7}$$

IECNORM.COM : Click to view the full PDF of IEC TR 63307:2020

where

$$Z_{\mathrm{m}} = r_{\mathrm{m}} + \mathrm{j}\,x_{\mathrm{m}} =$$

$$r_{\mathrm{fixture}} + \mathrm{j}\,x_{\mathrm{fixture}} + r_{\mathrm{Short}} + \mathrm{j}\omega L =$$

$$r_{\mathrm{fixture}} + \mathrm{j}\,x_{\mathrm{fixture}} + r_{\mathrm{Short}} + \left(r_{\mathrm{NSS}} + \mathrm{j}\omega L_{\mathrm{NSS}} + \mathrm{j}\omega L_{\mathrm{Short}}\right) \tag{A.8}$$

$$Z_{\mathrm{sm}} = r_{\mathrm{sm}} + \mathrm{j}\,x_{\mathrm{sm}} =$$

$$r_{\mathrm{fixture}} + \mathrm{j}\,x_{\mathrm{fixture}} + r_{\mathrm{Short}} + \mathrm{j}\omega L_{\mathrm{Short}} \tag{A.9}$$

Then, the complex permeability is given by:

$$\mu_{\mathrm{r}} = \frac{2\pi}{\mu_0}\frac{Z_{\mathrm{m}} - Z_{\mathrm{sm}}}{\mathrm{j}\omega \mathrm{F}} + 1 = \frac{2\pi}{\mu_0}\frac{Z_{\mathrm{NSS}}}{\mathrm{j}\omega \mathrm{F}} + 1 \tag{A.10}$$

that is,

$$\mu'_{\mathrm{r}} = \frac{2\pi}{\mu_0}\frac{x_{\mathrm{m}} - x_{\mathrm{sm}}}{\omega \mathrm{F}} + 1 = \frac{2\pi}{\mu_0}\frac{x_{\mathrm{NSS}}}{\omega \mathrm{F}} + 1 \tag{A.11}$$

$$\mu''_{\mathrm{r}} = \frac{2\pi}{\mu_0}\frac{r_{\mathrm{m}} - r_{\mathrm{sm}}}{\omega \mathrm{F}} = \frac{2\pi}{\mu_0}\frac{r_{\mathrm{NSS}}}{\omega \mathrm{F}} \tag{A.12}$$

IECNORM.COM : Click to view the full PDF of IEC TR 63307:2020